Aerosol Science and Technology, 38:555–573, 2004

ISSN: 0278-6826 print / 1521-7388 online
DOI: 10.1080/02786820490465504

Chase Studies of Particulate Emissions from in-use New York City Vehicles

Manjula R. Canagaratna,[1] John T. Jayne,[1] David A. Ghertner,[2] Scott Herndon,[1] Quan Shi,[1] Jose L. Jimenez,[3] Philip J. Silva,[1] Paul Williams,[4] Thomas Lanni,[5] Frank Drewnick,[6] Kenneth L. Demerjian,[6] Charles E. Kolb,[1] and Douglas R. Worsnop[1]

[1]*Center for Aerosol and Cloud Chemistry and Center for Atmospheric and Environmental Chemistry, Aerodyne Research Inc., Billerica, Massachusetts*
[2]*University of California, Berkeley, California*
[3]*University of Colorado, Boulder, Colorado*
[4]*University of Manchester, Manchester, United Kingdom*
[5]*Department of Environmental Conservation, Albany, New York*
[6]*Atmospheric Sciences Research Center, State University of New York, New York*

Emissions from motor vehicles are a significant source of fine particulate matter (PM) and gaseous pollutants in urban environments. Few studies have characterized both gaseous and PM emissions from individual in-use vehicles under real-world driving conditions. Here we describe chase vehicle studies in which on-road emissions from individual vehicles were measured in real time within seconds of their emission. This work uses an Aerodyne aerosol mass spectrometer (AMS) to provide size-resolved and chemically resolved characterization of the nonrefractory portion of the emitted PM; refractory materials such as elemental carbon (EC) were not measured in this study. The AMS, together with other gas-phase and particle instrumentation, was deployed on the Aerodyne Research Inc. (ARI) mobile laboratory, which was used to "chase" the target vehicles. Tailpipe emission indices of the targeted vehicles were obtained by referencing the measured nonrefractory particulate mass loading to the instantaneous CO_2 measured simultaneously in the plume. During these studies, nonrefractory $PM_{1.0}$ ($NRPM_1$) emission indices for a representative fraction of the New York City Metropolitan Transit Authority (MTA) bus fleet were determined. Diesel bus emissions ranged from 0.10 g $NRPM_1$/kg fuel to 0.23 g $NRPM_1$/kg, depending on the type of engine used by the bus. The average $NRPM_1$ emission index of diesel-powered buses using Continuously Regenerating Technology (CRT™) trap systems was 0.052 g $NRPM_1$/kg fuel. Buses fueled by compressed natural gas (CNG) had an average emission index of 0.034 g $NRPM_1$/kg Fuel. The mass spectra of the nonrefractory diesel aerosol components measured by the AMS were dominated by lubricating oil spectral signatures. Mass-weighted size distributions of the particles in fresh diesel exhaust plumes peak at vacuum aerodynamic diameters around 90 nm with a typical full width at half maximum of 60 nm.

Received 27 February 2003; accepted 29 March 2004.

This work was supported in part by the New York State Energy Research and Development Authority (NYSERDA), contract # 4918ERT-ERES99; the US Environmental Protection Agency (EPA), cooperative agreement # R828060010; and New York State Department of Environmental Conservation (NYS DEC), contract # C004210. Although the research described in this article has been funded in part by US EPA, it has not been subjected to the Agency's required peer and policy review and therefore does not necessary reflect the views of the Agency, and no official endorsement should be inferred. The authors thank the MTA for their cooperation, including Chris Bush for providing bus fleet information and Dana Lowell for help in organizing the logistics of the Fall 2000 campaign, the NYS DEC for providing drivers during the chase experiments, and Queens College for logistical support during the Summer 2001 campaign. The TILDAS scientists on-board the mobile laboratory, particularly Joanne Shorter and Mark Zahniser, are acknowledged for their assistance throughout the two phases of this study. Thanks also go to Jay Slowik and Leah Williams for help with laboratory soot experiments, Tim Onasch for assistance with the development of data analysis programs, and Paul Ziemann for useful discussions about organic mass spectral analysis. P. J. Silva thanks the Camille and Henry Dreyfus Foundation for Support. D. A. Ghertner thanks Robert Harriss for providing funding for his involvement in this project.

Address correspondence to Manjula R. Canagaratna, Center for Aerosol and Cloud Chemistry and Center for Atmospheric and Environmental Chemistry, Aerodyne Research Inc., 45 Manning Road, Billerica, MA 01821, USA. E-mail: mrcana@aerodyne.com

INTRODUCTION

Urban and regional air pollution has a wide range of impacts including reduced visibility, acid deposition, and severe human health effects. Some of the largest sources of fine particulate matter (PM) pollution in an urban environment are heavy-duty

diesel vehicles such as trucks and buses. For example, although diesel-powered vehicles make up only a small fraction of the on-road vehicle fleet in California, the statewide emission inventory in 2000 indicates that they account for approximately 35% of statewide on-road PM_{10} emissions (California Air Resources Board 2001). Similarly, the US Environmental Protection Agency (EPA) reports indicate that 70% of all PM mobile emissions can be attributed to heavy-duty diesel vehicles (EPA 2000).

In order to reduce the detrimental effects of vehicle emissions, EPA has instituted emission regulations for total hydrocarbons, CO, NO_x, and total PM. These regulations place limits on the mass of emitted PM since this parameter is viewed as the best indicator of their potential impact on human health effects (Dockery et al. 1993; Pope et al. 2002). The EPA emission standards that will be phased in by 2007 in the U.S. represent a particularly stringent challenge for diesel engine manufacturers (EPA 2002). In response to the emission standards, engine manufacturers have made advances in various aspects of engine technology (Sawyer et al. 2000). Improvements that allow for the use of higher fuel-injection pressures and control of fuel-injection rate and timing, for example, have resulted in a significant lowering of PM emissions. While the emission of PM mass has been reduced in many of these engines, measurements indicate that they emit increased numbers of nanoparticles ($D_p < 50$ nm diameter), which contribute very little to PM mass (Kittelson 1998). Nanoparticles are of concern because of their increased lung deposition efficiency relative to larger particles (Kittelson 1998). Increasingly stringent standards have also led to the development and greater use of diesel exhaust aftertreatment systems such as oxidative particulate traps, and of alternative fuel and engine technologies such as compressed natural gas (CNG) and spark-ignition engines in heavy-duty vehicles.

Emission inventories for in-use fleets of heavy-duty diesel vehicles are currently obtained on the basis of engine certification data from engine dynamometer tests. The tests are conducted according to the Federal Test Procedure (FTP), which involves operation of the engine over a range of load and speed settings while the emissions are measured. The use of engine certification data results in a poor determination of the emission inventory of an in-use fleet of vehicles because operating conditions of engine dynamometer tests do not fully or accurately represent those that the engine experiences during on-road use in a vehicle. Moreover, mobile emissions are also sensitive to vehicle parameters such as age, maintenance, and chemical and physical properties of the fuel and lubricating oil, and to ambient conditions such as humidity, temperature, pressure (Gautam et al. 1992) and altitude (Bishop et al. 2001). Individual driving styles can have a further effect on vehicle emissions (Katragadda et al. 1993). Significant discrepancies between emission inventories and real-world emissions have been reported (Jimenez et al. 2000). Since emission inventories provide the foundations for control strategy policy, it is important to verify their accuracy by comparison with actual in-use vehicle fleet emissions. The uncertainties in the vehicle emission inventories were highlighted in the mobile source emission review sponsored by NARSTO, which states that "validation studies based on direct measurement of the in-use fleet need to be performed to assess the accuracy of the emissions models. Confidence in the inventory will remain low until agreement is obtained between top-down and bottom-up validation approaches" (Sawyer et al. 2000, p. 2179).

Characterization of mobile emissions from heavy-duty vehicles under more realistic in-use conditions has been performed via chassis dynamometer, tunnel, and remote sensing studies. This research area has been recently reviewed by Yanowitz et al. (2000). In a chassis dynamometer study, the vehicle is subjected to prescribed driving cycles that are designed to model typical driving conditions. It is important to note, however, that sensitivity to dynamometer drive cycle (Yanowitz et al. 2000) and exhaust dilution conditions (Abdul-Khalek et al. 1998) can introduce considerable variability in dynamometer measurements. These uncertainties, together with the typically low sample sizes (due to the high cost per test) of dynamometer studies limit the usefulness of these measurements for obtaining representative estimates for in-use emissions. Tunnel studies have overcome some limitations of dynamometer studies and have provided evidence of differences between gas phase emission inventories and actual emissions (Pierson et al. 1990). They have also been used to monitor PM emissions from diesel vehicles (Kirchstetter et al. 1999). While tunnel measurements provide average fleet emission values, they cannot provide insight into the degree and causes of emissions variability among different heavy duty diesel vehicles. In addition, since the measurement site and conditions in tunnel studies are usually fixed, these studies are necessarily limited to only selected traffic conditions and types of vehicles. Cross-road remote sensing studies have the advantage of measuring the emissions of a large number of individual vehicles, although each vehicle is only sampled at one operating condition. A remote sensing technique for detecting PM emissions based on exhaust opacity has been in use for a number of years (Stedman et al. 1997), but this measurement is poorly correlated with particle mass concentrations (Gautam et al. 2000). A number of other techniques are currently under development to address this problem, but they have yet to demonstrate their quantification potential under field conditions (Desert Research Institute 1999; McManus et al. 2002).

A recently developed approach for obtaining realistic emission estimates involves the use of a mobile laboratory to "chase" and measure emissions from in-use vehicles (Kittelson et al. 2000; Shorter et al. 2001). The particular advantages of the mobile sampling platform include its ability to study a statistically representative sample of vehicles for fleet characterization and its ability to sample each vehicle under many different real-world operating conditions. Mobile laboratories also allow for characterization of emission sources that are otherwise not accessible to conventional fixed location sampling sites. The mobile platform can be positioned upwind and downwind of sources to directly measure the impacts of emissions. A few examples

of mobile laboratory studies to measure vehicle exhaust and the spatial/temporal distribution of air pollutants have been reported in literature (Bukowiecki et al. 2002; Jimenez et al. 2000; Kittelson et al. 2000; Shorter et al. 2001). This article describes the application of a mobile laboratory platform for the determination of in-use vehicle PM emission indices.

The measurements presented in this article were obtained using the Aerodyne mobile laboratory, which was equipped with both gas and particulate instruments with the necessary time response and sensitivity to characterize dilute exhaust plumes. The mobile lab can be used to determine both the particulate and gas-phase contents of an exhaust plume. This article focuses on the nonrefractory PM emission measurements obtained with the Aerodyne aerosol mass spectrometer (AMS). Particle emission data obtained with a condensation particle counter (CPC) are also briefly discussed. The gas-phase measurements will be the subject of a separate publication. A preliminary account of the measured gaseous pollution (NO, NO_2, SO_2, CH_4) emission indices has been presented previously (Shorter et al. 2001).

The experiments described here were conducted as part of the CNG/CRT Emission Perturbation Experiment (CEPEX) during the PM2.5 Technology Assessment and Characterization Study in New York City (PMTACS-NY; PMTACS 2000). The study involved a two-week demonstration in October 2000, followed by a five-week intensive campaign in the summer of 2001. The goal of these experiments was to characterize new and existing bus engine technologies used by the NYC Metropolitan Transit Authority (MTA) and to contrast these with the rest of the New York City heavy-duty fleet. The classification of each MTA bus that was chased was made possible by a detailed database of vehicle and engine information that was provided by the MTA. During these studies, the entire MTA fleet of diesel buses was being operated with ultralow-sulfur diesel fuel (max 30 ppm S by weight). Both conventional diesel-powered buses as well as diesel buses using Continuously Regenerating Technology (CRT™ is a registered trademark of Johnson Matthey) particle filters, which involve trapping and oxidation of exhaust particles (Cooper and Thoss 1989), were studied. Buses using spark-ignition technology and alternative fuels such as CNG were also studied.

EXPERIMENTAL

Aerodyne Aerosol Mass Spectrometer

The Aerodyne AMS has been described in detail elsewhere (Jayne et al. 2000; Jimenez et al. 2003b; Drewnick et al. 2004b), and only a brief description will be given here. The AMS operates by using an aerodynamic lens (Liu et al. 1995a, 1995b; Zhang et al. 2002) to sample submicron particles into vacuum, where they are aerodynamically sized, thermally vaporized on a heated surface, and chemically analyzed via electron impact ionization quadrupole mass spectrometry. Results from measurements obtained at several fixed ground sites indicate that the AMS has the potential to quantitatively measure size-dependent mass concentrations of nonrefractory chemical species (including most organic carbon (OC) and inorganic (acid, salt) components) for the aerosol ensemble with some single-particle information (Allan et al. 2003b; Jimenez et al. 2003b).

The relationship between the vacuum aerodynamic diameter measured by the AMS and the mobility and classical aerodynamic diameters has been detailed in a recent publication (Jimenez et al. 2003a). The vacuum aerodynamic diameter (D_{va}) differs from the classical aerodynamic diameter (D_a) in that the former is measured when the expansion that results in the size-dependent particle velocity occurs under free-molecular regime particle flow conditions, while the latter occurs under continuum regime flow conditions. The relationship between the two diameters is as follows (Hinds 1999):

$$D_{va} = \sqrt{\frac{\rho}{\chi \rho_0}} D_a, \qquad [1]$$

where χ is the dynamic shape factor that accounts for particle asphericity, ρ is the density of the particle material, and ρ_0 is unit density (1 g cm^{-3}). This expression assumes that the dynamic shape factor for continuum flow conditions is the same as that for free molecular flow conditions.

The AMS is operated in two modes. In the time-of-flight (TOF) mode, aerosol size distributions are determined for several preselected fragment ions using a beam-chopping technique. In the mass spectrum (MS) mode, the chopper is used to intermittently block and open the particle beam, and ensemble mass spectra (m/z 0–300) are obtained for the sampled aerosol. During the CEPEX experiment the AMS was operated with a new fast data acquisition mode that enabled time-resolved measurements to be obtained over the sampling timescale of individual vehicle plumes. In this mode the AMS was alternated between the TOF and MS modes at 2 s intervals. Thus, mass spectra (0–300 amu) and chemically speciated particle size distributions were obtained with 2 s time resolution.

The electron impact ionization-based detection scheme used by the AMS requires aerosol species to be vaporized in order to be detected. Thus, this technique does not detect refractory components, where *refractory* is operationally defined to mean those species that evaporate slowly (t > a few seconds) at the temperature of the AMS vaporizer (~550 C). This corresponds to species that have very low vapor pressures at this temperature, such as mineral oxides or elemental carbon (EC) aerosols. However, volatile/semivolatile components internally mixed with refractory aerosol components can be detected by the AMS. For example, while recent measurements during the ACE-Asia campaign have shown that most mineral oxide particles could not be detected by the AMS, $Ca(NO_3)_2$ on these particles could be detected (Bower et al. 2002). Similarly, hydrocarbon compounds and PAHs usually associated with soot particles are also detected.

Mobile Laboratory

The ARI Mobile laboratory used in the studies reported here is built around a 1989 Ford Econoline 350 (gasoline powered) chassis with a gross vehicle weight of 4853 kg. The vehicle seats three people: a driver, a front-seat operator, and an instrument operator in the rear. The rear of the mobile lab is a "box" approximately 4.3 m L × 2.1 m W × 1.8 m H in size which houses all the instrumentation. When the truck is moving, the instrumentation is powered by a 5 kW gasoline fueled generator (Honda EZ5000) which is mounted to the rear bumper of the truck. While classified as a truck, the mobile lab is still sufficiently small and maneuverable to "chase" vehicles and to travel on narrow roadways. The layout for the Aerodyne Research Inc. (ARI) Mobile Laboratory, as deployed in New York City, is shown in Figure 1.

In addition to the AMS, the mobile lab was equipped with two ARI tunable infrared laser differential absorption spectroscopy (TILDAS) instruments utilizing lead salt diode lasers (Shorter et al. 2001; Zahniser et al. 1995) for real-time measurements of selected trace gases such as NO, NO_2, CO, N_2O, CH_4, SO_2, and H_2CO (formaldehyde). A commercial LICOR nondispersive infrared unit provided real-time CO_2 measurements. The mode in which the CO_2 analyzer was operated during this study allowed for the determination of CO_2-mixing ratios up to 4000 ppm with an accuracy of 6% and a 1 s RMS of 1.6 ppm. A commercial TSI Model 3022 CPC provided total number densities for particles with diameters between 7 and 2500 nm, and a video camera directed out the front windshield provided a multipurpose record of the less measurable parameters, such as automobiles slipping in between the bus and the mobile lab, or intersection crossings. An onboard Trimble Pro XR Global Positioning Sensor (GPS) provided a highly accurate record of the lab's position, while a shaft rotation counter attached to the driveshaft of the mobile van gave the lab velocity. Data from each individual instrument was logged on a central onboard computer, enabling all data streams to be viewed in real-time and stored synchronously.

Inlet System

For the two studies reported here, two different inlet systems were used, which reflected the development of the mobile lab platform. In the October 2000 study, which was the first deployment of the particle instruments onboard the mobile lab, two separate inlets were used, one for the particle instruments (AMS, and CPC) and one for the gas-phase instruments (TILDAS and LICOR). The inlet system used in the July 2001 deployment was

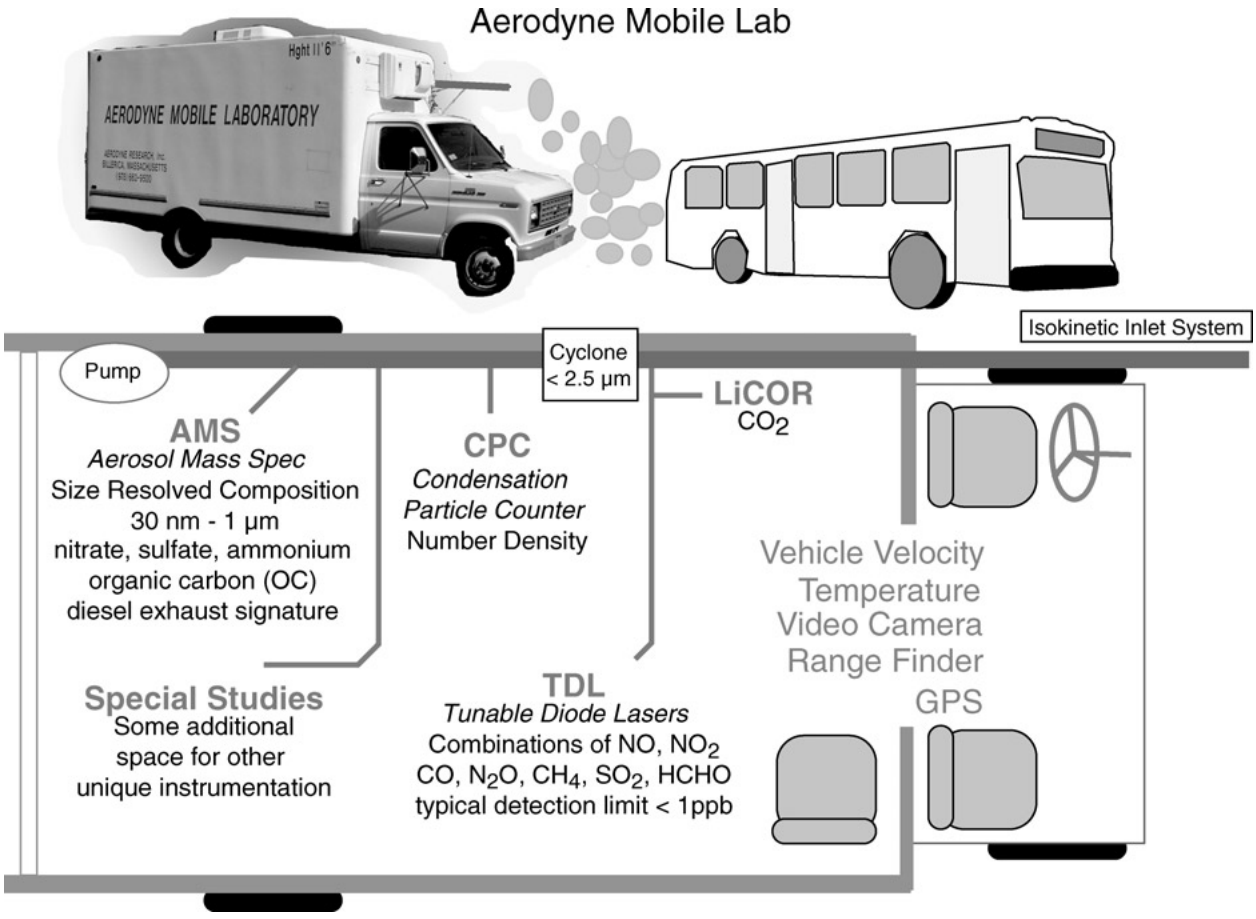

Figure 1. Schematic of the ARI mobile laboratory as instrumented for the CEPEX/PMTACS-NY experiment.

a "common inlet" design from which both the gas and particle instruments drew their sample. The height of both inlet systems from road level was 2.4 m. Only the relevant features of the inlet systems that served the particle instruments will be described here.

In the October 2000 deployment the main aerosol sample flow for the AMS and CPC was drawn into the mobile lab through a 0.64 cm ID copper tube that protruded 5 cm through the forward bulkhead of the cabin (driver side, colocated with the gas-phase instrument inlet). The total length of the 0.64 ID copper tube from the bulkhead of the truck to the AMS was 4.3 m. The total flow through this tube was 10 l min^{-1} (LPM). This flow passed through a cyclone separator (URG model 509) that provided a 2.5 micron cut to remove larger particles. Isokinetic flow separation was performed downstream of the cyclone to provide 87 cm^3 min^{-1} to the AMS and 300 cm^3 min^{-1} to the CPC. The remaining 9.6 LPM was exhausted to the sampling pump.The measured average inlet residence or "lag" time for the aerosol between entering the main inlet of the mobile lab and being detected by the AMS was 7 s. The temperature of the sampled air was measured in the gas-phase inlet line.

During the July 2001 deployment a common inlet was employed for both the gas and particle instruments. The common inlet was a 2.11 cm ID stainless steel tube that protruded forward from the driver-side bulkhead. The total flow through this common inlet was 18.9 LPM. Of this total flow, 10 LPM was isokinetically split and delivered to the cyclone separator and aerosol instruments; the remaining 8.9 LPM was diverted to the gas-phase instruments. The flows to the cyclone, the AMS, and the CPC, as well as the isokinetic sampling points, were identical to the October 2000 deployment inlet system. It is important to note that while the splitting of flows from the common inlet is performed in an isokinetic manner, the sampling of gas into the common inlet itself was not designed to be isokinetic. However, even at speeds of 30 m/s, when the inlet is subisokinetic, negligible inertial losses are calculated for particles less than 1 micron in size (Hinds 1999).

The 2.11 cm ID main inlet tube extended 1.2 m forward of the bulkhead. The longer inlet was used to provide sufficient time for laminar flow to develop prior to the flow splitter, to avoid possible vehicle boundary layer sampling artifacts at the mobile lab bulkhead, and to get the inlet closer to top-emitting diesel buses. Sample temperature was measured at the center of the 2.11 cm ID tube just prior to the gas-particle flow split. A comparison of the maximum gas and PM signal levels measured with the summer 2001 and fall 2000 inlets indicates that the longer common inlet system resulted in increased signal intensity for top-emitting buses, but an approximately 30% reduction in signal intensity (due to sampling of a less-concentrated plume region) for downward-(street-level) emitting buses.

The particle transmission efficiency of the July 2001 inlet system was measured using 350 nm diameter NH_4NO_3 aerosol generated using an atomizer differential mobility analyzer (DMA) combination. In this test, the DMA output aerosol was delivered to the front of the mobile lab inlet with the CPC colocated to provide a number density measurement. Particle-free air was used to make up the total inlet flow. The CPC count rate was compared to the AMS count rate, and they agreed to within 15% after accounting for flow dilution. It was concluded that for this size particle there was no significant aerosol loss, and as a result no corrections were made to the data to account for inlet transmission. Calculated estimates of particle loss for smaller-size aerosol (down to 30 nm) due to gravitational settling, impaction, and diffusion are less than 1% (Hinds 1999). Particle losses were not measured at particle sizes other than 350 nm. No measurements were made to determine the transmission efficiency of the fall 2000 deployment inlet system; however, it should have been at least as good as that used in the summer 2001 system since the external inlet was shorter and the particle subsampling system was identical.

Chase Experiments

During the CEPEX study a typical chase experiment involved following a selected vehicle at a distance of approximately 3–15 m with the Aerodyne mobile lab while the target vehicle drove through city traffic or through quiet neighborhoods, making stops to pick up or discharge passengers. Except for a few cases, drivers of the target vehicles were not aware that their vehicle's emissions were being measured, and thus the driving conditions and style encountered in this study can be assumed to be representative of typical conditions. Target vehicles were chosen randomly among heavy-duty vehicles, with preference given to MTA buses since a fleet characterization of these vehicles was desired. A database provided by the MTA, which, contained vehicle information such as engine type, age, and fuel by bus number, was used to categorize each MTA bus. Automated preliminary analysis of the data was used to display the results of the emission measurements in real time on the on-board computers. Chases of an individual vehicle generally ranged from 4–7 min with the duration of a chase being decided by scientists aboard the mobile laboratory. This decision was based on the measurement of a sufficient number of intense CO_2 plumes ($\Delta CO_2 > 250$ ppm) from the target vehicles or the inability to maintain the chase due to vehicle cutoffs and heavy traffic. The start and end points of the chase together with notes on the drive conditions and pertinent chase details were written to text files and automatically tagged with the appropriate time for later use during data analysis.

DATA ANALYSIS

Determination of PM Mass from AMS Signals

As mentioned earlier, refractory materials do not produce ion signals in the AMS. Thus, only nonrefractory components of exhaust aerosol are determined in this study, although measured vacuum aerodynamic diameters reflect the presence of both the refractory and nonrefractory particle components. Theoretical

calculations indicate a 50% transmission efficiency cutoff for the aerodynamic lens at around 700 nm. Recent lab measurements suggest that the actual 50% transmission efficiency cutoff is closer to 1000 nm (Zhang et al. 2002). Thus, according to our best estimates, the measured volatile aerosol mass reported here is representative of $NRPM_1$. The mass spectra measured during the vehicle chases were used to calculate sulfate, organic, and total $NRPM_1$ mass in the exhaust. The conversion of AMS mass spectral signals to mass loadings has been described in previous publications, so a detailed discussion of this topic will not be repeated here (Allan et al. 2003a; Jimenez et al. 2003b). Briefly, TOF or MS ion signals from a given species are summed together and are then converted to mass loadings ($\mu g\ m^{-3}$) using instrument calibrations of the ionization and collection efficiencies for that species.

The ionization efficiency of the AMS was calibrated nearly every day using a primary aerosol standard, NH_4NO_3. Mass loadings for other species can be calculated in terms of the calibrated ionization efficiency of the NO_3^- moiety of NH_4NO_3 and a species-specific correction factor that can be measured in the laboratory (Jimenez et al. 2003b). A detailed description of the AMS ionization efficiency calibration procedures is the subject of another manuscript in preparation. Previous studies of heavy-duty diesel engine exhaust aerosols have shown that under typical operating conditions most of the NRPM organic aerosol mass is accounted for by unburned lubricant oil and diesel fuel (Tobias et al. 2001) Studies in our lab on atomized diesel fuel and lubricant oil aerosol have measured the ionization efficiency of volatile oil/fuel organic species to be twice as large as that of NO_3^- with a measurement uncertainty of $\pm 17\%$. This factor of 2 is used together with the daily calibrations of NO_3^- ionization efficiencies to calculate the mass of the organic PM in diesel exhaust. Similarly, a factor of 1.51, determined from previous lab and field studies (Drewnick et al. 2004b; Hogrefe et al. 2004), was used for the calculation of SO_4^{-2} loadings. This factor accounts for both the ionization efficiency of SO_4^{-2} relative to NO_3^- and the fact that we do not regularly use all observed SO_4^{-2} fragment ions in the calculation of the SO_4^{-2} mass concentrations.

Collection efficiency refers to the fraction of sampled particles that impact on the hot AMS vaporizer. Since only particles that reach the vaporizer contribute to the measured signal in the AMS, if the collection efficiency of the sampled particles onto the vaporizer is not unity, it is necessary to correct the measured mass by a factor that accounts for collection losses. The aerodynamic lens focuses sampled spherical particles into a narrow particle beam such that their collection efficiency on the vaporizer is 100% (Zhang et al. 2002); nonspherical particles, however, are not focused as well by the aerodynamic lens, and this could lead to less than 100% collection efficiencies. Previous studies have shown that the measured PM mass in heavy-duty vehicle exhaust is primarily accounted for by particles with physical diameters in the 50–500 nm size range that have a soot core (Kittelson et al. 2000). Experiments in our lab with propane flames have produced two types of soot with apparently different morphologies: one type has a 100% collection efficiency in the AMS, while the other has a collection efficiency as low as 50% because it is not well focused. The degree to which the focusing behavior of these propane soot types resemble that of organic-covered soot particles emitted by diesel engines is not definitively known. Thus, the mass loading calculations in this study were performed with an assumed collection efficiency of 100% and should be taken as a lower limit of the actual aerosol mass. Variations in the morphologies of emitted particles could result in the need to use different AMS collection efficiencies for the calculation of emission indices across various vehicle types. Since these AMS collection efficiency differences have not yet been experimentally determined, we further make the assumption of using a 100% collection efficiency for the particles emitted by all vehicle types measured in this study.

Reasonable extremes for the possible AMS ionization and collection efficiencies of emission aerosols, when taken together, result in a maximum uncertainty in the calculated AMS mass loading of $+140\%$ and -14%. This is the dominant source of uncertainty in the accuracy of the emission indices reported in this article. Experiments involving uncoated and coated soot aerosols that more directly quantify the ranges of collection and ionization efficiencies of exhaust aerosol are currently being developed in our laboratory. The possibility of examining these issues during chassis or engine dynamometer emission studies is also being explored. Furthermore, the installation of a beam width probe within the AMS (Jayne et al. 2000) for continuous measurement of particle collection efficiency is being tested. Based on the anticipated results of these developments, we expect that the uncertainties in calculated AMS mass loadings during future emission measurement campaigns will be significantly reduced.

Synthesis of Vehicle Chase Event Data

The term "vehicle chase event" is used in this manuscript to refer to the entire time period during which a single target vehicle was chased by the mobile lab. The calculation of $NRPM_1$ emission indices for a single vehicle begins with the synthesis of the time trends of continuously measured AMS data together with the other data collected on the mobile lab during the chase event for that particular vehicle. Figure 2 shows the AMS time trend of total $NRPM_1$ as well as analogous trends in the 1 s measurements of CO_2 mixing ratio, total particle number concentration, and mobile lab speed during a single vehicle chase event. The mobile lab speed is used as a proxy for the target vehicle's speed. The baseline signal levels in the gas and particle time trends represent ambient concentrations of the various species during the chase event. The sharp dip in CO_2 concentration at 5:50 pm corresponds to a time period when N_2 was blown through the sampling inlet to measure zero-signal background levels for the various instruments. The peaks in the particle and gas-phase signals, which usually last for approximately 10–20 s, represent separate instances during the chase when the sampling

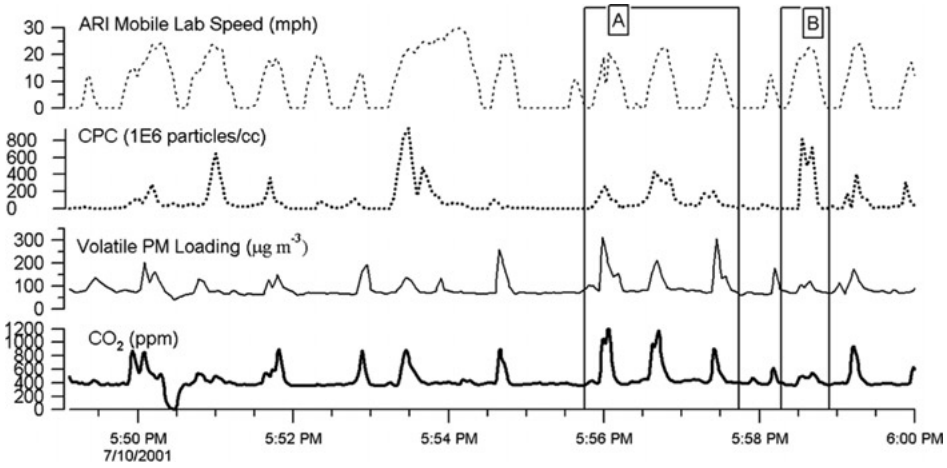

Figure 2. Example of chase event data obtained while following an individual vehicle with the mobile laboratory. The $NRPM_1$ loadings are obtained with the AMS. Each peak in the CO_2 signal signifies a "capture" of the target vehicle's exhaust plume. The valleys between plume captures reflect ambient gas and PM loadings. The sharp dip in the CO_2 concentration arises from one of a series of periodic N_2 purges of the inlet system that were used to measure background signal levels in the various instruments.

inlet of the mobile lab captured the single target vehicle's exhaust plume. Thus, a single vehicle chase event is made up of a series of "plume captures" that reflect the emissions of the target vehicle under a range of driving conditions.

The correlation between the changes in the particle and CO_2 concentrations are evident in Figure 2. The correlation between PM and CO_2 is essential to this experiment because CO_2 is used as a tracer for the exhaust plume. The CO_2 concentration in raw gasoline exhaust, which contains a stoichiometric amount of air, is ~12.4% or 124,000 ppm. Diesel engines always operate with an excess of air, and the CO_2 concentration in diesel exhaust ranges between ~2–3% at low power and 10% at high power (Heywood 1988). Levels of CO_2 sampled in this study ranged from 100 to 800 ppm, indicating that plumes were diluted by a factor of 25–1000 by the time they entered the inlet of the mobile laboratory. It is known from dilution tunnel studies of vehicle exhaust that while particle size distributions change during the plume-dilution process, particle mass is conserved (Kittelson 1998).

As in tunnel and remote-sensing studies, we assume that, since dilution is controlled by turbulent mixing, the different pollutants emitted by the vehicle are diluted to the same extent over the sampling volume. In this way we can calculate a PM emission index that is referenced to CO_2. This CO_2-based emission ratio can then be converted to a fuel-use–based emission index, because CO_2 emissions are proportional to fuel burned. Strict accounting of exhaust carbon species would require the addition of CO and total hydrocarbon (THC) emissions to CO_2, but it is known that for diesel vehicles these emissions are generally too small to significantly affect the carbon balance (Yanowitz et al. 2000).

Since CO_2 is emitted by all mobile sources on the road, it is important to differentiate CO_2 plume captures that belong to the vehicle of interest from those that belong to other vehicles and remove them from the emission index calculation. The identification of contaminated plume captures was primarily accomplished with the video images and operator notes that were obtained for each chase event. The video images were used to gauge traffic level and to check for time periods in which other vehicles physically entered the space between the target vehicle and the mobile lab. Self-contamination from the exhaust of the gasoline-powered ARI mobile lab is a valid concern (especially during low mobile lab speeds), but it appeared to have a negligible effect during this study. Although self-contamination cannot be determined from the video images, it could be identified during diesel vehicle chases because the NO_X/CO_2 ratio in plume captures from gasoline- and diesel-powered vehicles are distinctly different from each other. During CRT™ vehicle chases, clear differences in NO_2/NO_x emission ratios between standard diesel and CRT™-equipped diesels were similarly useful in providing additional confirmation about the source of the various plume captures.

Peaks in PM loading that occurred with no corresponding increase in CO_2 or that occurred during time periods when other sources of PM can be identified in the video images are automatically removed from the chase event analysis.

Calculation of Emission Ratios

The methods used to calculate PM emission ratios for each vehicle chase event varied slightly between the two measurement phases of this experiment. Intercomparisons between these methods over hundreds of chase events indicate that the two analysis methods agree to within 15% with no systematic deviation. While the emission ratios calculated from both of these methods have combined measurement precision and emission variability on the order of 10–20%, it is important to note that the accuracy with which these emission ratios are calculated is limited, as described earlier, by the absolute accuracy with which the AMS

ionization efficiency and collection efficiencies for combustion particles are known.

1. Method 1: For the first phase of the measurement campaign (fall 2000) the net change in PM concentration over the entire chase event relative to ambient background levels was divided by the corresponding change in CO_2 to yield an emission ratio (ER) of $NRPM_1/CO_2$ in units of $\mu g\ m^{-3}$/ppm as follows:

$$ER = \sum_{i=StartTime}^{i=EndTime} (PM_i - PM_{bgd}) \Big/ \sum_{i=StartTime}^{i=EndTime} (CO_{2i} - CO_{2bgd}). \quad [2]$$

The baseline ambient levels for each of these species were determined from time periods immediately before and after each chase event when the mobile lab was not directly following any vehicles and was driving in the immediate neighborhood of the relevant chase event.

2. Method 2: The data from the summer 2001 experiments were analyzed by performing a linear fit of the PM mass versus CO_2 concentration over the entire chase event. Figure 3 shows this procedure applied to the chase event data shown in Figure 2. The linear fit is performed with the intercept fixed at representative ambient CO_2 and PM values for the event. Since more than 50% of the time during most vehicle chase events is spent measuring the ambient background (i.e., the valleys in between the peaks in Figure 2), the PM and CO_2 concentrations that were sampled most frequently during the chase were used as representative ambient background values for each of these species. For chase events that were short or did not have adequate time spent sampling background levels, ambient concentrations for each of these species were determined from appropriate time periods immediately before and after the chase event.

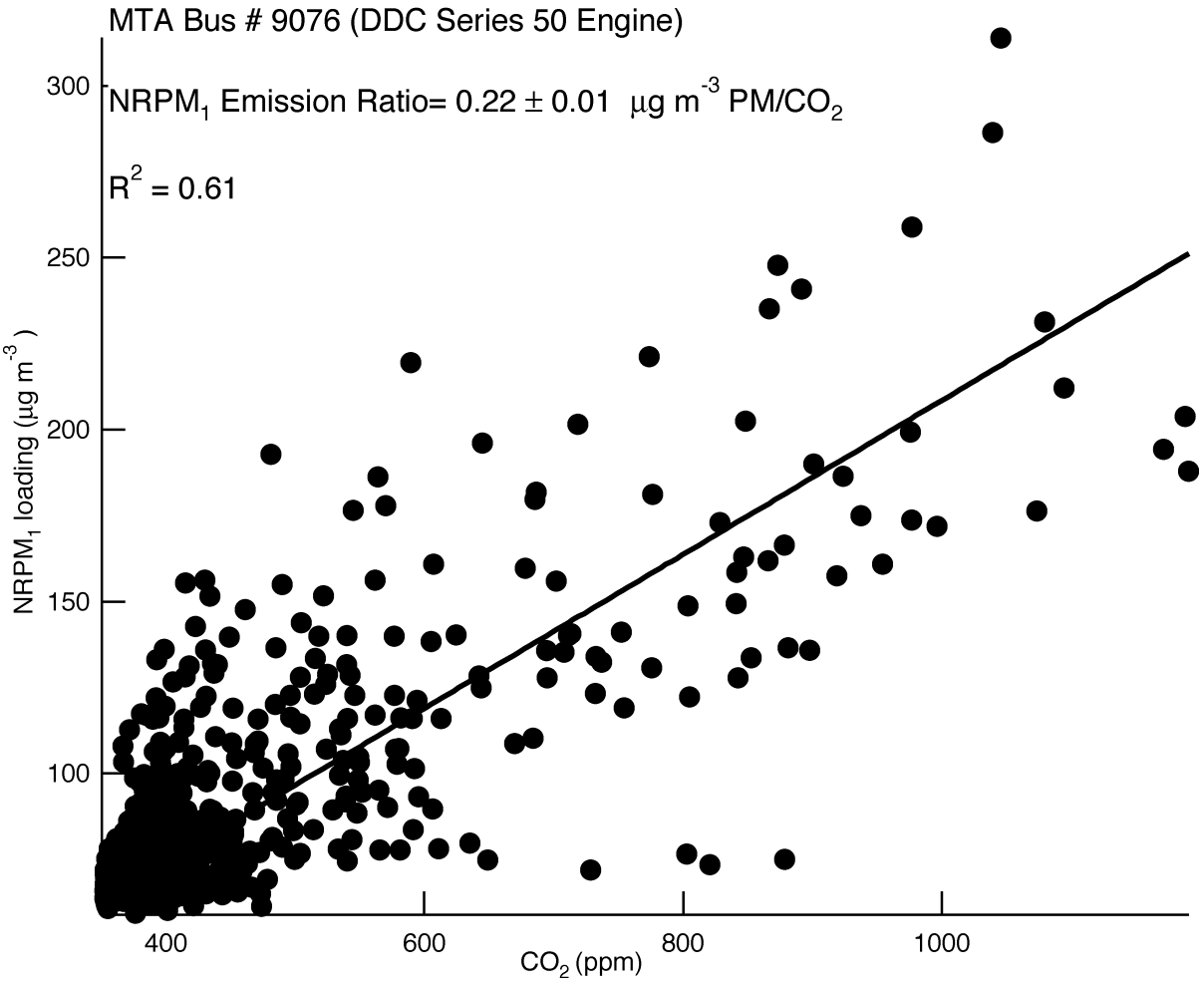

Figure 3. The correlation between PM and CO_2 signals is used to obtain emission ratios in units of $\mu g\ m^{-3}$ $NRPM_1$/ppm CO_2. The data in this figure is fit to a straight line passing through a fixed intercept corresponding to the ambient background PM and CO_2 concentrations, which were determined as described in the text.

The sensitivity of the exhaust plume PM measurements was determined from noise levels in the AMS time variation of aerosol mass during chase event time periods when the ambient background was being continuously sampled for at least 30 s. This yields 2 s sensitivities (S/N = 3 in 2 s) of 6 μg m^{-3} and 7.5 μg m^{-3} for sulfate and $NRPM_1$ mass, respectively, which correspond to sensitivities of 0.015 and 0.019 μg m^{-3}/ppm for a typical vehicle plume CO_2 concentration increase of 400 ppm. Since these sensitivity values are determined by ion counting (of background ions in the vacuum chamber) and particle counting (dominated by sampling rate of ambient particles) statistics, they decrease as a function of $1/\sqrt{}$sampling time. Thus, the actual detection limits for these species will be considerably lower when averaged over many plume captures and many vehicle chase events. For example, on average the total time spent capturing vehicle plumes in any individual 5 min long chase event is about 50 s. If 100 of these individual chase events are averaged together, then the sensitivities would be 50 times lower than the 2 s sensitivity values quoted above.

The single emission ratio determined from a chase event represents the average PM emission characteristics of the given vehicle over the entire measurement time period. For the chase event shown in Figure 2 and analyzed in Figure 3, for example, the fitted emission ratio is 0.22 μgm^{-3}/ppm CO_2, with a linear least-squares fit uncertainty of 10% (2 σ. The 2 σ fit uncertainties ranged from 4–18% for all vehicle chase events in this study. Since the fitted data for these chase events include many data points with background CO_2 levels (i.e., $\Delta CO_2 < 250$ ppm) and small degrees of scatter, these fit uncertainties are likely lower limits of the combined true measurement precision and emission variability of the emission ratio measurements. For example, when the data in Figure 3 is fitted again with only "intense" CO_2 plume data (i.e., $\Delta CO_2 > 250$ ppm), an ER value of 0.21 μgm^{-3}/ppm CO_2 with an increased uncertainty of 20% is obtained. Unfortunately, since the buses that were chased in this study were chosen on a random basis to maximize the number of sampled vehicles, the same vehicle was not typically measured on different days, and thus the repeatability of measured emission indices was not routinely assessed. However, it is of interest to note that for 4 individual buses, each of which was chased on 2 separate occasions, the respective emission ratios determined from the separate measurements agreed to within 15%.

Some of the variability in the measured emission ratio for a given vehicle appears to be due to variations in instantaneous driving conditions during the chase event. For example, in the chase event shown in Figure 2, high particle mass and high particle number emission regimes appear to alternate during vehicle operation (compare time trends of CPC particle number concentration with trends in AMS mass concentration in sections A and B of Figure 2). The anticorrelation of AMS and CPC signal intensities in these sections can be explained by the fact that the particle number is most sensitive to changes in the number of small (7–50 nm) particles, while particle mass is sensitive to changes in the number of larger (50–500 nm) particles.

The emission ratios (ER) that are obtained in units of μg m^{-3} $NRPM_1$/ppm CO_2 can be converted to emission indices (EI) in the more standard units of g $NRPM_1$/kg fuel by multiplying them by a factor of 1.77. This factor is derived by using the following equation:

$$EI = (ER/490.8)(10^3)(W_c), \quad [3]$$

where the division of the emission ratio by 490.8 is used to convert the CO_2 concentration from units of ppm to units of μg of carbon m^{-3}, and W_c is the weight fraction of carbon in diesel fuel. A typical W_c value of 0.87 is used in the calculations (Heywood 1988; Kirchstetter et al. 1999).

RESULTS AND DISCUSSION

Comparison of Emission Indices Measured for Different Vehicle Types

Figure 4 summarizes the results of all the emissions indices calculated in this study categorized by vehicle type. The height of each bar denotes the average emission index calculated over all chase events for that particular vehicle class while the error bar represents one standard error of the mean. The vehicle classes are broadly categorized as MTA buses, non-MTA buses, and other heavy-duty vehicles. Within the MTA fleet, buses were divided into diesel, CRT^{TM}, and CNG categories, with each diesel bus being further separated according to the Detroit Diesel Corporation (DDC) engine model (6V-92 or Series 50) it used. The "non-MTA buses" category consists of transit buses used in the city that are operated by companies other than the MTA. The "other heavy-duty" vehicle category contains trucks as well as school and charter buses. The emission indices calculated for a car emitting a large amount of blue smoke, and for mixed-traffic plumes in a few tunnels are also shown in the figure.

Diesel Vehicle Emissions

The MTA diesel bus fleet has average emissions of 0.12 and 0.25 g $NRPM_1$/kg fuel for the Series 50 and 6V-92 engine technologies, respectively. These engine models, which are manufactured by the DDC, are widely used in bus fleets (Prucz et al. 2001). The 6V-92, a common transit bus engine produced during the 1980s, is a two-stroke engine model. The Series 50 is a newer four-stroke engine model that has been widely used in transit buses since 1993. Figure 5 shows the variability in measured emission indices of MTA diesel buses as a function of engine model year. The figure indicates that, on average, all model years of the Series 50 engine emit less PM than the 6V-92 models. Moreover, buses with Series 50 engines have a smaller range of scatter in PM emissions than those with 6V-92 engines.

Recently, Prucz et al. (2001) published a comprehensive analysis of the Series 50 and 6V-92 bus engine chassis dynamometer measurements performed over the last decade. The dynamometer data, which was obtained with a commercial business district

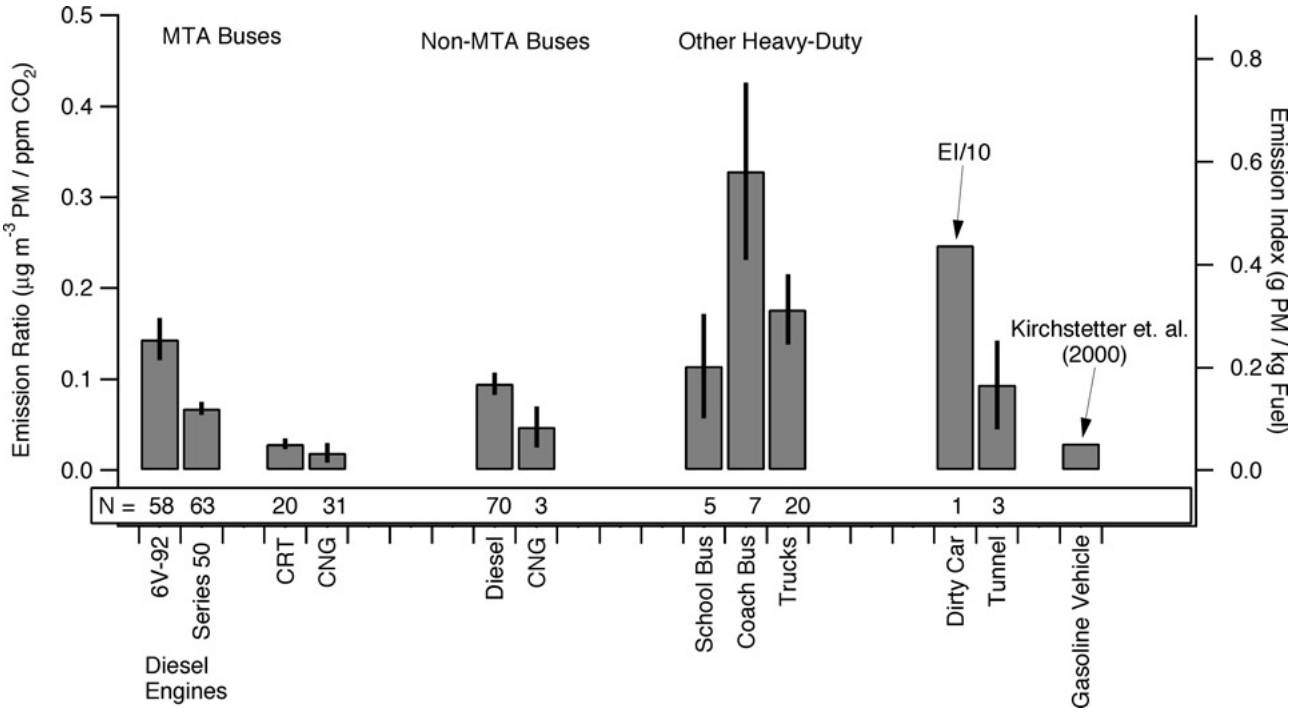

Figure 4. Classification of average nonrefractory PM emissions by vehicle type. The height of each bar reflects the average emission index calculated over all the relevant chase events that represent the particular vehicle class. The error bar represents ±1 standard error of the mean.

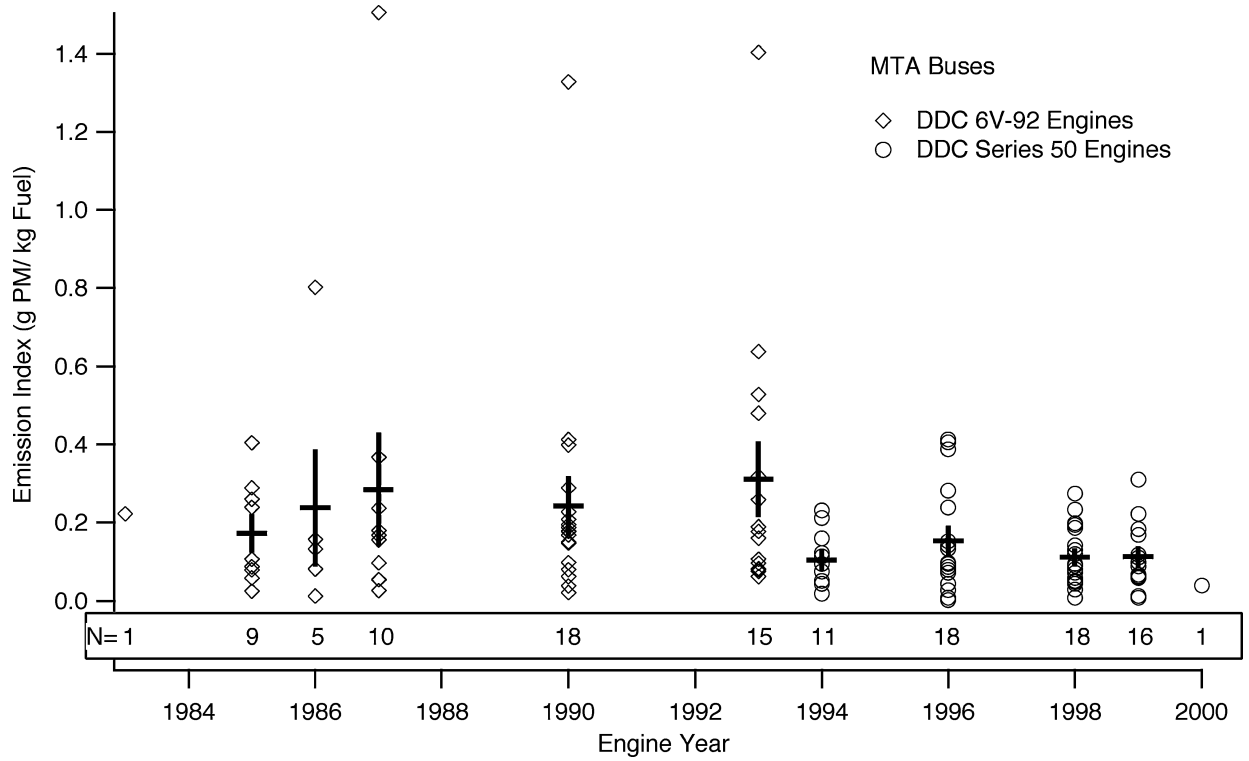

Figure 5. Comparison of MTA diesel bus emissions by engine year and model. The 6V-92 DDC engine is an older model than the Series 50 DDC engine. The horizontal lines show the emission index averages for each engine model year and the vertical lines reflect ±1 standard error of the mean.

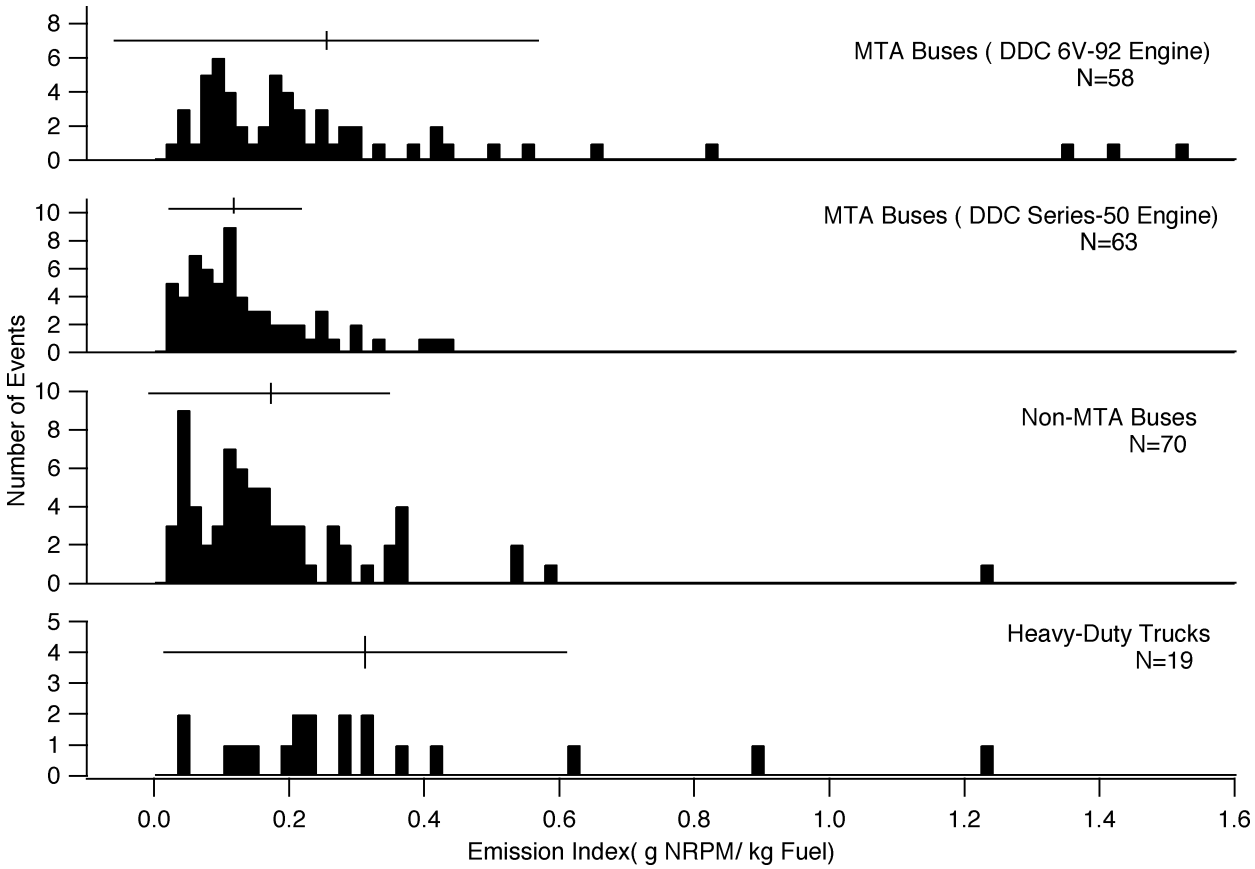

Figure 6. Frequency distribution of emission indices measured within different heavy-duty diesel vehicle categories. The average emission index for each vehicle class and one standard deviation of the associated measurements are indicated by the vertical and horizontal lines above each histogram.

(CBD) dynamometer drive cycle, shows a reduction in the PM mass emissions and emission scatter for Series 50 engines compared to 6V-92 engines, though the 70% reduction measured in the dynamometer studies is larger than the 50% $NRPM_1$ mass emission reduction measured by the AMS in the current study. This difference may reflect the difference in $NRPM_1$ measurement by the AMS compared to total PM (including soot) in the dynomometer studies, or it could be related to differences in drive cycle and vehicle operating conditions in the two studies. The dynamometer studies also show a clear reduction in PM emissions as a function of year (particularly for the 1990–1992 6V-92 engines), which was not observed in this study. This comparison may be limited by the counting statistics of the current AMS study which, for example, included 15–18 measurements for each of the 1990–1992 6V-92 model engine years, compared to the dynomometer studies which had an average of 100 individual measurements for each model year obtained over many years.

Since the engine model/year information used to analyze the MTA diesel bus measurements was not available for the non-MTA diesel transit buses, only one average emission index of 0.16 g/kg fuel emission was obtained for this category. This emission index is similar to the 0.17 g/kg fuel average emission index calculated for the entire MTA diesel fleet. The EI for transit buses appear to be similar to those of school buses (0.19 g/kg fuel) and lower than those of coach buses measured in this study (0.56 g/kg fuel). The emission indices of the transit buses are also approximately 50% smaller than the heavy-duty trucks (EI = 0.30 g/kg fuel) sampled during this study. For comparison, chassis dynamometer studies have shown a 40% reduction in emissions of buses compared to heavy-duty trucks. It is important to note that, although average values are presented for each of these vehicle classes, considerable scatter in emission values was observed within each class. For example, frequency distributions of individual vehicle emission index measurements within the MTA 6V-92, MTA Series 50, non-MTA buses, and trucks are shown in Figure 6. It is likely that the variability seen within each vehicle category is a reflection of the complex dependence of mobile source emissions on factors such as vehicle age, engine model, maintenance, and driving conditions.

Table 1
Comparison of emission data from present study with previous tunnel and chassis dynamometer studies

Reference	Approach	Location	Year sampled	PM measurement method	Vehicle type	OC (g/kg fuel)	EC (g/kg fuel)	PM (g/kg fuel)
This work	Mobile lab	New York City	2000, 2001	AMS (1.0 μ cut)	MTA buses	0.12–0.25	—	—
				AMS (1.0 μ cut)	Non-MTA bus	0.17	—	—
				AMS (1.0 μ cut)	Trucks	0.37	—	—
Kirchstetter et al. (1999)	Tunnel	Caldecott Tunnel	1997	Filter (2.5μ cut)	Trucks	0.5	1.3	2.5
Allen et al. (2001)	Tunnel	Caldecott Tunnel	1997	Filter (1.9μ cut)	Trucks	0.43 [b]	0.68	1.11
Lowenthal et al. (1994)	CD[a]	Phoenix	1992	Filter (2.5μ cut)	Trucks/buses	0.6[c]	1.3	2.2
Yanowitz et al. (2000)	CD[a]	Multiple	—[d]	Filter (2.5μ cut)	Trucks	0.4–0.9[e]	—	2.26[f]
					Buses	0.3–0.5[e]	—	1.35[f]
Prucz et al. (2001)	CD[a]	Multiple	1992–99	Filter (2.5μ cut)	Buses	0.3–0.6[e]	—	1.54[g]

[a] Chassis Dynamometer Studies.
[b] Converted from units of mg/kg C by using a diesel fuel carbon weight fraction of 0.87.
[c] Converted from units of mg/km by using an assumed fuel efficiency of 5.5 g/l.
[d] This analysis includes published and unpublished CD data from more than 250 different vehicles. The dates on which these studies were conducted were not published in the referenced manuscript.
[e] OC fraction estimated from total PM by using OC fractions measured in Kirchstetter et al. (1999) and Allen et al. (2000).
[f] Converted from units of g/gal by using a diesel fuel density of 840 g/l.
[g] Converted from units of g/mile by using an assumed fuel efficiency of 5.5 g/l.

Table 1 shows a comparison of the $NRPM_1$ emission values determined in this study with PM, OC, and EC emission values determined by tunnel studies (Allen et al. 2000; Kirchstetter et al. 1999) and chassis dynamometer studies (Prucz et al. 2001; Yanowitz et al. 2000). The conversion factors used to transform emission ratios reported in the original papers into the g/kg fuel units can be found in the table legend. In the two tunnel studies the exhaust particles were collected on filters for total mass measurement as well as for speciation in terms of OC and EC. Both of these measurements indicate that 20–40% of the total PM mass is in the form of organic carbon. Other studies report OC fractions of 30–40% for heavy-duty diesel trucks (Hildermann et al. 1991; Lowenthal et al. 1994). As already mentioned above, the AMS is sensitive only to nonrefractory components of sampled aerosol. Therefore, the AMS measured mass is most directly comparable to the OC mass measured in these previous studies. Although the Lowenthal et al. (1994) study reports OC emission measurements, the other 2 chassis dynamometer studies in Table 1 measured total PM mass without further speciation of the aerosol mass. In order to compare these latter results with the AMS measurements, a range of expected OC mass was estimated for each of these measurements by multiplying the total PM emissions by 20–40% (the fraction of OC observed in previous studies).

The average $NRPM_1$ emission index measured by the AMS for transit buses is lower than the OC emissions estimated for buses from the dynamometer PM measurements shown in Table 1 (Prucz et al. 2001; Yanowitz et al. 2000). Similarly, the PM_1 emission index measured for trucks by the AMS is smaller than the OC emissions measured in the two tunnel studies (Allen et al. 2000; Kirchstetter et al. 1999) and the Lowenthal et al. (1994) study shown in Table 1. In the Allen et al. (2001) tunnel study, $PM_{1.9}$ emissions were found to be about 50% of PM_{10} emissions. Thus, it was suggested that the differences between the PM emission indices reported by the tunnel studies of Allen et al. (2001) and Kirchstetter et al. (1999) could be due to the mass that was not captured in a $PM_{1.9}$ measurement compared to a $PM_{2.5}$ measurement. This argument may explain why the AMS nonrefractory PM_1 emission measurements for trucks and buses is lower than the previously measured and estimated OC values. The assumption of unit AMS collection efficiency for the nonspherical exhaust particles may also result in low values for emission indices measured by the AMS. Differences in the vehicles and driving conditions sampled by the mobile van, truck, and chassis dynamometer experiments could also account for some of the discrepancies.

In addition to total $NRPM_1$, the sulfate concentration and size distribution of the diesel exhaust aerosol were also monitored

by the AMS. The measured sulfate emission values for the individual MTA buses resulted in a fleet average sulfate emission ratio of 0.0003 ± 0.0003 μg m^{-3}/ppm CO_2. The measured average sulfate emission ratios for non-MTA diesel buses and trucks were 0.002 ± 0.001 μg m^{-3}/ppm CO_2 and 0.003 ± 0.002 μg m^{-3}/ppm CO_2, respectively. The higher sulfate emissions from these non-MTA vehicles is not surprising since they were likely using standard on-road diesel fuel with about 350 ppm S fueled as opposed to the ultralow sulfur fuel (<30 ppm S by weight) used by the MTA. These values for non-MTA diesels and trucks are reasonably consistent with chassis dynamometer studies by Yanowitz et al. (1999), which report sulfate emission indices of 0.06 g/gal (0.001 μg m^{-3}/ppm CO_2) for a variety of heavy-duty vehicles operated with 300 ppm S fuel. The Yanowitz et al. (1999) study also reports that the sulfate emission indices measured between different heavy-duty vehicles is variable and not always correlated with total PM emissions.

Emissions from Alternative Technologies

Measured emission indices of CRT-equipped diesel buses and CNG-fueled buses were 0.052 g $NRPM_1$/kg fuel and 0.034 g $NRPM_1$/kg fuel, respectively. When compared with respect to two standard errors of their reported means, the emission indices of the CNG and CRT-equipped buses measured in our chase study do not differ significantly from each other. It is interesting to note, as shown in Figure 4, that the emission indices of CRT^{TM} and CNG buses are very similar to those reported for light-duty gasoline vehicles in the Kirchstetter et al. (1999) tunnel study in California.

The CRT^{TM} is a passive emission control system that combines an oxidation catalyst and a filter to reduce PM emissions. It uses NO_2 produced by oxidation of the NO already present in vehicle exhaust to burn soot collected by the filter at the typical operating temperatures of diesel exhaust. It requires the use of ultralow sulfur fuel (approximately 30 ppm S) for maximum performance (Chatterjee et al. 2001). A previous chassis dynamometer study of 2 MTA Series 50 diesel buses operating with and without CRTs indicates that the particle trap reduces total PM mass by 88% and 83% with respect to standard buses fueled with 350 ppm S and 30 ppm S fuel, respectively (Chatterjee et al. 2001). This total PM reduction is accomplished by a ~90% reduction in the soot (BC) fraction and a ~60–80% reduction in the OC fraction of exhaust PM (Fujii et al. 2002; Gibbs 2000). Since the AMS measurements reflect only changes in nonrefractory PM components like OC, the 57% reduction (with respect to Series 50 powered buses) measured in this study appears to be consistent with the lower limit of this previous work. Chassis dynamometer tests report that CNG and CRT-equipped buses have similar EC/OC ratios in their PM emissions (Lanni et al. 2002) and similar PM emission reductions with respect to diesel baseline cases (Holmen and Ayala 2002; Lanni et al. 2002). The chase measurements performed in this study are in agreement with the latter observations.

Other Events

While PM emissions from gasoline vehicles were not explicitly pursued in this study, it is of interest to note that the vehicle with the largest emission index measured in this study was a gasoline-fueled car that was emitting plumes of bluish gray smoke. The latter observation is usually associated with vehicles that are burning lubricant oil. As shown in Figure 4, the emission index of this car is approximately 10–20 times greater than the diesel vehicles measured in this study, and about 100 times greater than that measured for light-duty gasoline vehicles in tunnel studies. While this large emission index is surprising, measurements of gas-phase emissions from gasoline vehicles have also shown that a small fraction of the vehicles can account for a large fraction of the fleet emissions (Bishop et al. 1996; Jimenez et al. 1999, 2000). From this standpoint, it appears that this car is an example of a PM superemitter within the gasoline light-duty fleet.

Figure 4 also shows an average of AMS vehicle emission measurements from 3 different NYC tunnels. These measurements were conducted under mixed-traffic conditions (i.e., gasoline and diesel vehicles), and no attempt was made to count the number of vehicles of each category for this analysis. In general, medium traffic conditions were encountered in the tunnels, and no single vehicle was followed. Thus, the AMS and CO_2 signals increased steadily upon entry of the tunnel and decreased abruptly upon exit of the tunnel. For each tunnel, the emissions were calculated as an average of the net change in $NRPM_1$ mass divided by the net change in CO_2 concentration during the drive through the tunnel. Since the numbers of gasoline and diesel-vehicles were not counted, the conversion from CO_2 to fuel was performed using diesel conversion factors. The average emission index measured under these conditions is similar to the average emissions measured from the diesel powered MTA buses.

CHARACTERIZATION OF DIESEL PARTICLES

Chemical Composition

Most of the previous studies of the chemical composition of diesel exhaust particles have involved the collection of the particles on filters during chassis dynamometer or tunnel tests followed by solvent extraction and GC-MS analysis of the resulting chemical species (Kleeman et al. 2000; Rogge et al. 1993; Schauer et al. 1999) In filter-based studies only 5–15% of the elutable particulate mass is typically resolved and speciated. The rest of the eluted particulate mass is referred to as unresolved complex mixture (UCM) and is not speciated. This UCM is known to consist mostly of branched and cyclic hydrocarbons (Rogge et al. 1993) and to be similar to motor oil components (Schauer et al. 1999). This is consistent with other studies that have shown that unburned lubricating oil and fuel account for

a large fraction of the volatile diesel exhaust aerosol (Sakurai et al. 2003; Tobias et al. 2001).

The dominant organic components of fuel and lubricating oil are n-alkanes, branched alkanes, cycloalkanes, and aromatics (including polyaromatic hydrocarbons). Differences in processing of fuel and lubricating oil result in diesel fuel being enriched in n-alkanes, while the lubricating oil contains relatively more cycloalkanes and aromatics (Tobias et al. 2001). Measurements of nanoparticles emitted by a heavy-duty diesel engine operating under heavy- and light-load lab conditions show that different hydrocarbon enrichments in diesel and lubricating oil result in differing mass spectra (Tobias et al. 2001). These measurements used a thermal desorption particle beam mass spectrometer (TDPBMS; Tobias et al. 2000), which involves vaporization of collected aerosol followed by electron impact ionization and quadrupole mass spectrometry of the resulting gas-phase species. In another recent TDPBMS study, by ramping the temperature at which the aerosol was vaporized and using mass spectral matching techniques the volatile component of both diesel nanoparticles and larger particles was determined to be at least 95% unburned lubricating oil (Sakurai et al. 2003).

Since the detection schemes used by the AMS and TDPBMS are nearly identical, the TDPBMS mass spectra spectral signatures can be used to distinguish fuel and lubricant oil in this analysis. Figures 7a, 7b, and 7c show AMS mass spectra of diesel bus exhaust, lubricant oil, and diesel fuel aerosols, respectively. The diesel bus exhaust spectrum is an average of exhaust mass spectra obtained during the diesel vehicle chase events sampled in this study; each chase event exhaust spectrum was obtained by subtracting the average ambient background mass spectrum obtained during the event from the average plume capture mass spectrum. The lubricant oil and diesel fuel AMS spectra were obtained from lab aerosols by cooling the hot oil or diesel vapor and atomizing the diesel fuel. All spectra in Figure 7 are dominated by the ion series $C_nH^+_{2n+1}$ (m/z 29, 43, 57, 71, 85, 99 . . .), which is typical of normal and branched alkanes; in addition, the series $C_nH^+_{2n-1}$ (m/z 27, 41, 55, 69, 83, 97, 111 . . .) and $C_nH^+_{2n-3}$ (m/z 67, 79, 81, 95, 107, 109 . . .), typical of cycloalkanes, and $C_6H_5C_nH^+_{2n}$ (m/z 77, 91, 105, 119 . . .), typical of aromatics, are observed (McLafferty and Turecek 1993; Tobias et al. 2001).

In the Tobias et al. (2001) study, the ratio of the alkane to cycloalkane series in the m/z 41–43, 53–57, 67–71, and m/z 81–85 ranges was used to distinguish the condensed lubricant oil/fuel ratio in the aerosol. In particular, the increasing dominance of the cycloalkane series compared to the normal/branched alkane series within the m/z 67–71 and m/z 81–85 ranges was used as a strong signature of a high lubricant oil/unburned fuel ratio. This trend is observed in both the pure lubricant oil and diesel exhaust spectra shown in Figure 7. This indicates, as observed in previous TDPBMS studies (Sakurai et al. 2003; Tobias et al. 2001), that under most operating conditions the organic carbon fraction of in-use diesel vehicle exhaust aerosol is dominated by condensed lubricating oil.

Size Distribution

In the TOF mode, the AMS measures chemically speciated mass distributions as a function of the vacuum aerodynamic diameters of particles. Previous studies have shown that diesel exhaust particle size distributions are typically trimodal with a small nanomode (0–50 nm), an accumulation mode (50–500 nm), and a coarse mode ($>1\mu$m) (Kittelson 1998). While the nanomode particles dominate number-weighted size distributions and have received a great deal of attention recently because of the high efficiency with which they deposit in the respiratory tract, the accumulation-mode particles account for most of the $PM_{2.5}$ mass and dominate mass-weighted size distributions. The coarse mode can account for 5–20% of the PM_{10} mass (Kittelson 1998). Since the AMS provides mass-weighted size distributions and has less than 50% lens transmission efficiency for particle diameters larger than 1 μm, it is most sensitive to the accumulation mode of the exhaust aerosol.

Figure 8 shows an average of the chemically resolved size distributions provided by the AMS during the chase event shown in Figure 3. The sulfate and organic size distributions shown in the figure were obtained by averaging TOF-mode measurements for representative sulfate ion fragments (m/z = 48(SO^+), 64 (SO_2^+)) and organic ion fragments (m/z = 55, 57, 95, 107). Since the fragments monitored in the TOF-mode account for only a fraction of all the sulfate and organic ion fragments, the average size distributions obtained from the representative fragments were then normalized to reflect the total mass of each species observed in the MS-mode. For each species, separate size distribution averages were obtained according to a CO_2 concentration-based data-processing filter that distinguished "in-plume" (plume capture) sampling from ambient background aerosol sampling. The "in-plume" and background size distributions are plotted as solid and dotted curves, respectively, in Figure 8. Because of the large dilution experienced by the exhaust plume when it exits the tailpipe, even the "in-plume" size distributions are a combination of both exhaust and ambient aerosol distributions. For example, in Figure 8, the larger mode (vacuum aerodynamic diameter ~400 nm) of the "in-plume" sulfate distribution is dominated by ambient aerosols, but the smaller mode (~90 nm) is dominated by vehicle emissions. The small mode is also prominent in the "in-plume" organic distribution, and comparison with the background organic distribution indicates that this mode is largely due to exhaust aerosol.

For each event, an "exhaust only" aerosol size distribution can be obtained by taking the difference between the solid and dotted lines for each species. Averages of the chemically speciated "exhaust only" size distributions measured during diesel chase events sampled in this study are shown in Figure 9. The theoretically calculated transmission efficiency of the aerodynamic lens as a function of vacuum aerodynamic diameter is also plotted in the figure for reference. Both the average sulfate and organic distributions have a small mode peaking between 90–100 nm and a larger mode that peaks around 550 nm. The sharp drop-off in intensity of the large mode for diameters >600 nm is likely due

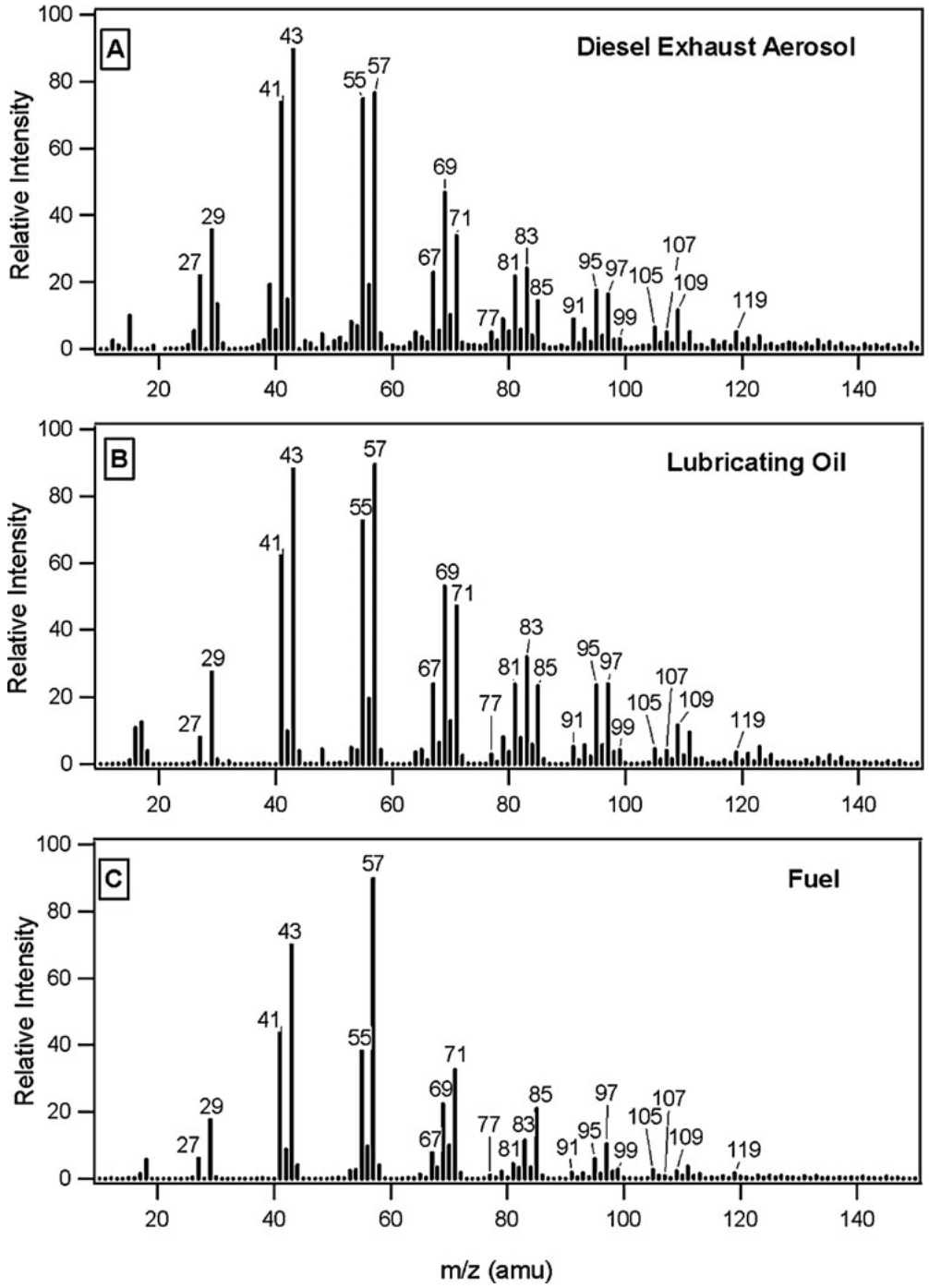

Figure 7. AMS mass spectra obtained for (a) diesel bus exhaust, (b) pure lubricant oil, and (c) pure diesel fuel aerosols. The lubricant oil and diesel fuel spectra were obtained from lab aerosols and the diesel bus exhaust spectrum is an average of PM exhaust mass spectra obtained during the diesel vehicle chase events sampled in this study.

to the analogous drop in the transmission efficiency of the lens for those diameters. The similarity of the sulfate and organic size distributions suggests that the two species are internally mixed in the exhaust aerosol. The AMS cannot definitively confirm the state of mixing, however, because it measures the ensemble aerosol rather than single particles. It is also interesting to note that since there is a clear separation in the aerodynamic diameters of the vehicle emission and ambient aerosol modes, integration of the exhaust-only size distributions over the small emission mode could provide an alternate, and possibly less noisy, means of obtaining vehicle sulfate emission mass values for emission ratio determination.

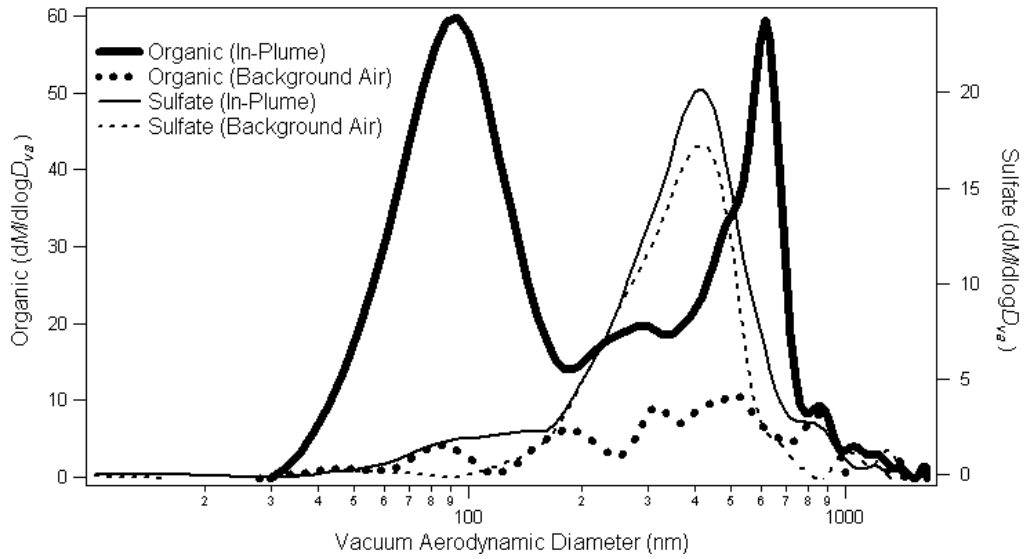

Figure 8. Chemically speciated size distributions measured for an individual vehicle during one chase event. The solid lines correspond to distributions averaged over time periods when the mobile laboratory was sampling the vehicle's exhaust plume. The dotted lines correspond to size distribution averages over time periods corresponding to ambient measurement conditions.

Although the distributions in Figure 9 represent averages over many diesel vehicles, driving conditions, and exhaust plume ages, the small organic mode was consistently observed in all diesel chase-event plume captures with peak positions generally ranging from 80–110 nm. Mobility sizing experiments indicate that the accumulation mode of the diesel exhaust mass size distribution typically peaks at a mobility diameter of around 100–200 nm (Kittelson 1998; Kleeman et al. 2000). A recent study shows that diesel particles with mobility diameters in the 100–200 nm range have classical aerodynamic diameters ranging from approximately 80–110 nm (Park et al. 2003). These classical diameters can be converted to vacuum aerodynamic diameters by using Equation (1) with appropriate density and dynamic shape factors. McMurry et al. (2002) measured effective

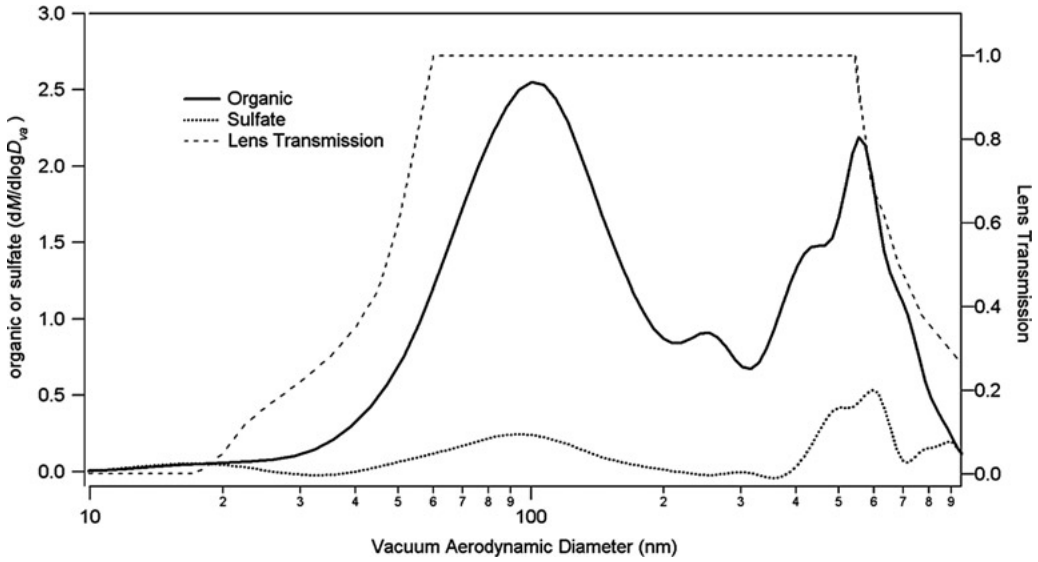

Figure 9. Average organic and sulfate "exhaust only" size distributions for diesel vehicle chase events. The "exhaust only" size distributions for each diesel chase event were calculated by taking the difference between the in-plume and background size distributions of each species. See text for details. The calculated transmission efficiency curve for the aerodynamic lens used in this study is also shown for reference. It is important to note, however, that recent lab measurements suggest that the actual 50% transmission efficiency cutoff is closer to 1000 nm.

densities for atmospheric particles with 107 and 309 nm mobility diameters and estimated shape factors for the smaller particles that were hypothesized to be due to vehicle emissions. For the 107 nm particles, dynamic shape factor ranges of 1.8–2.1 and 1.2–1.5 were estimated for assumed particle material densities of 2 g cm^{-3} and 1 g cm^{-3}, respectively. With these values and the results of the previous studies mentioned above, the exhaust aerosol mass-weighted size distribution is expected to peak at a vacuum aerodynamic diameter range of 75–135 nm. The small-mode peak measured by the AMS at 80–110 nm is consistent with this calculated range.

The particles that belong to the 500 nm mode in Figure 9 did not consistently appear in all chase-events or even all chase event plume captures, and no clear correlation was found between their appearance and the absolute emission index of the chase event or vehicle driving conditions. Previous studies indicate that coarse-mode particles are formed by re-entrainment of particles that had been deposited on cylinder and exhaust system surfaces (Kittelson 1998) and that there is no relationship between particle emission levels in the coarse modes and in smaller size modes (Morawska et al. 1998). The variability with which the 500 nm particles were observed suggests that they may be produced by a mechanism that is similar to the coarse-mode particles. However, further work is needed to identify the possible source of these particles.

Influence of Diesel Exhaust on Ambient PM Measurements in Urban Areas

Typical ambient aerosol size distributions measured by the AMS are bimodal (Allan et al. 2003a, 2003b; Jimenez et al. 2003b). Large (>200 nm) particles, which are composed of oxidized organic/sulfate mixtures, are observed in both rural and urban environments and appear to be associated with regional evolution and transport of aerosol. On the other hand, small organic particles (<200 nm diameter) are consistently observed in urban areas and appear to have a local source. For example, during the PMTACS-NY study, a second AMS, which was measuring ambient aerosol, showed that the average mass distribution of organic particles had two modes with maxima at 80 and 360 nm (Drewnick et al. 2004a). The relative importance of the small organic mode was generally correlated with traffic activity levels, and when the small mode was more intense than the large mode the measured ambient aerosol mass spectra resembled that shown in Figure 7b. These observations suggest that the small organic mode observed in urban ambient aerosol measurements is a signature of motor-vehicle–related aerosol. Studies are underway to combine the results of this in-use vehicle study with ambient AMS measurements to quantitatively evaluate the contribution of vehicle particle emissions to ambient aerosol loadings.

SUMMARY

In this study the Aerodyne mobile laboratory was used to chase individual vehicles and measure their emissions under real-world conditions. An innovative, fast-response AMS was used to measure the nonrefractory PM emission indices and to provide size and chemically resolved characterization of the nonrefractory fraction of exhaust PM. The nonrefractory diesel exhaust PM appears to be dominated by lubricating oil and the typical measured mass distribution of organic as well as sulfate species in diesel exhaust PM peak at vacuum aerodynamic diameters of ~90 nm.

In order to provide a fleet characterization of MTA buses, PM emission indices for 121 diesel-fueled, 20 CRT-equipped diesels, and 31 CNG-fueled buses were measured during this study. In addition to MTA buses, emissions from a variety of other individual transit buses and heavy-duty vehicles in the general New York City traffic mix were also measured. The measurements indicate that MTA diesel buses with newer Series 50 engines emit less $NRPM_1$ than older 6V-92 engines. The CRT-equipped and CNG-fueled buses have similar $NRPM_1$ emission indices and on average emit about 60% less $NRPM_1$ mass than Series 50 buses. However, the simultaneous gas-phase measurements obtained in this study, which will be presented in a separate publication, show that these reductions in PM emissions are accompanied by increased NO_2/NO_x ratios in CRT-equipped buses and increased CH_4 and CH_2O emissions from CNG buses. Thus, the evaluation of the usefulness of these technologies will have to take into account not only their effect on PM mass emissions but also their effect on gas-phase emissions. Moreover, since there is a continuing discussion about whether PM mass is the best metric of aerosol health effects, a comparison of these technologies should also take into account the size distributions and chemical characteristics of the emitted PM.

The results of this chase study are in reasonable agreement with previous measurements obtained from dynamometer and tunnel studies. This study has demonstrated some of the advantages of the chase method, including the ability to quickly study a large sample of vehicles for fleet characterization, the flexibility to sample a range of heavy-duty vehicles, and the ability to sample each vehicle under different real-world operating conditions. Moreover, it is important to note that the chase method has the potential of enabling the detailed study of the dependence of emission variability on vehicle driving conditions. Since the instruments on-board the mobile laboratory have fast time resolution, emission index differences between different plume captures of the same vehicle can be correlated with changes in operating conditions such as vehicle state (as approximated by the mobile laboratory's own speed) and grade of the road (from GPS measurements). This type of analysis has not been completed for this dataset, but it will be explored in the future. Since the AMS is not capable of measuring refractory material such as EC, which can account for approximately 50% of the emitted PM mass, particle instruments sensitive to soot will be added to the mobile laboratory instrument suite for future chase studies. Nanoparticle number density measurements will also be included in order to complement the AMS measurements

and provide a more complete characterization of the exhaust PM.

REFERENCES

Abdul-Khalek, I., Kittelson, D. B., Graskow, B. R., Wei, Q., and Brear, F. (1998). Diesel Exhaust Particle Size: Measurement Issues and Trends, *Soc. Automotive Eng.* 991142:1–9.

Allan, J. D., Coe, H., Bower, K., Williams, P. I., Gallagher, M. W., Alfarra, M. R., Jiménez, J. L., Worsnop, D. R., Jayne, J. T., Canagaratna, M. R., Nemitz, E., and McDonald, A. G. (2003a). Quantitative Sampling Using an Aerodyne Aerosol Mass Spectrometer, 1, Techniques of Data Interpretation and Error Analysis, *J. Geophys. Res.* 108:4090. DOI: 10.1029/2002JD002358.

Allan, J. D., Jiménez, J. L., Coe, H., Bower, K. N., Williams, P. I., Gallagher, M. W., and Worsnop, D. R. (2003b). Quantitative Sampling Using an Aerodyne Aerosol Mass Spectrometer, 2, Measurements of Fine Particulate Chemical Composition in Two UK Cities, *J. Geophys. Res.* 108:4091. DOI: 10.1029/2002JD002359.

Allen, J. O., Fergenson, D. P., Gard, E. E., Hughes, L. S., Morrical, B. D., Kleeman, M. J., Gross, D. S., Galli, M. E., Prather, K. A., and Cass, G. R. (2000). Particle Detection Efficiencies of Aerosol Time of Flight Mass Spectrometers under Ambient Sampling Conditions, *Env. Sci. Tech.* 34:211–217.

Bishop, G. A., Morris, J. A., Stedman, D. H., Cohen, L. H., Countess, R. J., Maly, P., and Scherer, S. (2001). The Effects of Altitude on Heavy-Duty Diesel Truck On-road Emissions, *Environ. Sci. Technol.* 35:1574–1578.

Bishop, G. A., Stedman, D. H., and Ashbaugh, L. L. (1996). Motor Vehicle Emissions Variability, *J. Air Waste Manag. Assoc.* 46:667–675.

Bower, K. N., Choularton, T. W., Coe, H., Allan, J. D., Burgess, R., Facchini, M. C., Alfarra, M. R., Topping, D., Williams, P. I., and McFiggans, G. B. (2002). Aerosol-Cloud Interactions in ACE-Asia, In *Abstracts of the 21st Annual AAAR Conference*, 128.

Bukowiecki, N., Kittleson, D. B., Watts, W. F., Burtscher, H., Weingartner, E., and Baltensperger, U. (2002). Real-Time Characterization of Ultrafine and Accumulation Mode Particles in Ambient Combustion Aerosols, *J. Aerosol Sci.* 33:1139–1154.

California Air Resources Board. (2001). *California Almanac of Emissions and Air Quality, 2001*.

Chatterjee, S., Conway, R., Lanni, T., Tang, S., Frank, B., Rosenblatt, D., Bush, C., Lowell, D., Evans, J., McLean, R., and Leavy, S. (2001). Performance and Durability Evaluation of Continuously Regenerating ParticulateFilters on Diesel Powered Urban Buses and NY City Transit_Part II. *SAE Technical Paper Series*, 2002-01-0430.

Cooper, B., and Thoss, J. (1989). Role of NO in Diesel Particulate Control. In *SAE Technical Paper Series* 890404.

Desert Research Institute. (1999). Fall Newsletter. Available at *http://newsletter.dri.edu/1999/fall/snaqs.html*

Dockery, D. W., Pope, C. A., Xu, X. P., Spengler, J. D., Ware, J. H., Fay, M. E., Ferris, B. G., and Speizer, F. E. (1993). An Association Between Air-Pollution and Mortality in 6 United States Cities, *N. Eng. J. Med.* 329:1753–1759.

Drewnick, F., Jayne, J. T., Canagaratna, M. R., Worsnop, D. R., and Demerjian, K. L. (2004a). Measurement of Ambient Aerosol Composition during the PMTACS-NY 2001 using an Aerosol Mass Spectrometer, Part II: Chemically Speciated Mass Distributions, *Aerosol Sci. Technol.* 38:104–117.

Drewnick, F., Schwab, J. J., Jayne, J. T., Canagaratna, M., Worsnop, D. R., and Demerjian, K. L. (2004b). Measurement of Ambient Aerosol Composition during the PMTACS-NY 2001 using an Aerosol Mass Spectrometer, Part I: Mass Concentrations, *Aerosol Sci. Technol.* 38:92–103.

Environmental Protection Agency (EPA). (2000). National Emission Inventory. Available at *http://www.epa.gov/ttn/chief/trends/trends00/trends2000.pdf*

Environmental Protection Agency (EPA). (2002). Diesel Exhaust in the United States. Available at *http://www.epa.gov/otaq/retrofit/documents/f02048.pdf*

Fujii, T., KIkezawa, H., and Kotani, Y. (2002). A Study on the Analysis of PM Components with CR-DPF. In *SAE Technical Paper Series*, 2002-01-1686.

Gautam, M., Byrd, R. L., Carder, D. K., Banks, P. D., and Lyons, D. (2000). Particulate Matter Emissions and Smoke Opacity from In-Use Heavy-Duty Vehicles, *J. Environ. Sci. Health Part A-Toxic/Hazardous Substances Environ. Eng.* 35:557–573.

Gautam, M., Ferguson, D. H., Wang, W. G., Bata, R. M., Lyons, D. W., Clark, N. N., Palmer, G. M., and Katragadda, S. (1992). *SAE Technical Paper Series*, 921751.

Gibbs, R. (2000). Un-Regulated Emissions from CRT-Equipped Transit Buses. *6th Diesel Engine Emissions Reduction Workshop*, August 20–24, San Diego, CA.

Heywood, J. B. (1988). Internal Combustion Engine Fundamentals. McGraw-Hill, Inc., New York.

Hildermann, L. M., Markowski, G. R., and Cass, G. R. (1991). Chemical Composition of Emissions from Urban Sourcesof Fine Organic Aerosol, *Env. Sci. Tech.* 25:744–759.

Hinds, W. C. (1999). Aerosol Technology: Properties, Behavior, and Measurements of Airborne Particles. John Wiley & Sons, Inc., New York.

Hogrefe, O., Drewnick, F., Lala, G. G., Schwab, J. J., and Demerjian, K. L. (2004). Development and Operation of an Aerosol Generation, Calibration and Research Facility, *Aerosol Sci. Technol.* 38:196–214.

Holmen, B., and Ayala, A. (2002). Ultrafine PM Emissions from Natural Gas, Oxidation-Catalyst Diesel, and Particle-Trap Diesel Heavy-Duty Transit Buses, *Env. Sci. Tech.* 36:5041–5050.

Jayne, J. T., Leard, D. C., Zhang, X., Davidovits, P., Smith, K. A., Kolb, C. E., and Worsnop, D. R. (2000). Development of an Aerosol Mass Spectrometer for Size and Composition Analysis of Submicron Particles, *Aerosol Sci. Technol.* 33:49–70.

Jimenez, J. L., Cocker, D. R., Bahreini, R., Zhuang, H., Varutbangkul, V., Flagan, R. C., Seinfeld, J. H., Hoffmann, T., and O'Dowd, C. (2003a). New Particle Formation from Photooxidation of Diiodomethane (CH2I2), *J. Geophys. Res.—Atmos.* 108:4318. DOI: 10.1029/2002JD002358.

Jimenez, J. L., Jayne, J. T., Shi, Q., Kolb, C. E., Worsnop, D. R., Yourshaw, I., Seinfeld, J. H., Flagan, R. C., Zhang, X., Smith, K. A., Morris, J., and Davidovits, P. (2003b). Ambient Aerosol Sampling Using the Aerodyne Aerosol Mass Spectrometer, *J. Geophys Res.* 108:8425. DOI: 10.1029/2001JD001213.

Jimenez, J. L., McRae, G. J., Nelson, D. D., and Zahniser, M. S. (2000). Remote Sensing of Heavy Duty Diesel Truck NO and NO2 Emissions Using Tunable Diode Lasers, *Environ. Sci. Technol.* 32:2380–2387.

Jimenez, J. L., Nelson, D. D., Zahniser, M. S., Koplow, M. D., and Schmidt, S. E. (1999). Characterization of On-Road Vehicle NO Emissions by a TILDAS Remote Sensor, *J. Air Waste Manag. Assoc.* 49:463–470.

Katragadda, S., Bata, R. M., Wang, W. G., Gautam, M., Clark, N., Lyons, D., Palmer, G. M., Stanley, S., Dunlap, L., Pellegrin, V., Wilson, R., and Porter, H. (1993). A Correlation Study Between Two Heavy-Duty Vehicle Chassis Dynamometer Emissions Testing Facilities. In *SAE Technical Paper Series* 931788.

Kirchstetter, T. W., Harley, R. A., Kreisberg, N. M., Stolzenburg, M. R., and Hering, S. (1999). On-Road Measurement of Fine Particle and Nitrogen Oxide Emissions from Light and Heavy-Duty Motor Vehicles, *Atmos. Env.* 33:2955–2968.

Kittelson, D. (1998). Engines and Nanoparticles: A Review, *J. Aerosol Sci.* 29:575–588.

Kittelson, D., Johnson, J., Watts, W., Wei, Q., Drayton, M., and Paulsen, D. (2000). Diesel Aerosol Sampling in the Atmosphere, *SAE Technical Paper Series*, 2000-01-2212.

Kleeman, M. J., Schauer, J. J., and Cass, G. R. (2000). Size and Composition Distribution of Fine Particulate Matter Emitted from Motor Vehicles, *Env. Sci. Tech.* 34:1133–1142.

Lanni, T., Frank, B. P., Tang, S., Rosenblatt, D., and Lowell, D. (2002). Performance and Emissions Evaluation of Compressed Natural Gas and Clean Diesel Buses and New York City's Metropolitan Transit Authority, *SAE Technical Paper Series* 2003-01-0300.

Liu, P., Ziemann, P. J., Kittleson, D. B., and McMurry, P. H. (1995a). Generating Particle Beams of Controlled Dimensions and Divergence: I. Theory of Particle Motion in Aerodynamic Lenses and Nozzle Expansions, *Aerosol Sci. Tech.* 22:293–313.

Lowenthal, D. H., Zielinska, B., Chow, J. C., Watson, J. G., Gautam, M., Ferguson, D. H., Neuroth, G. R., and Stevens, K. D. (1994). Characterization of Heavy-Duty Diesel Vehicle Emissions, *Atmos. Env.* 28:731–743.

McLafferty, F. W., and Turecek, F. (1993). Interpretation of Mass Spectra. University Science Books, Mill Valley, CA.

McManus, J. B., Nelson, D. D., and Zahniser, M. (2002). Development of a Laser Remote Sensing Instrument for PM and NO_x. *12th CRC On-Road Vehicle Emissions Workshop*, April 15–17, San Diego, CA.

McMurry, P. H., Wang, X., Park, K., and Ehara, K. (2002). The Relationship Between Mass and Mobility for Atmospheric Particles—A New Technique for Measuring Particle Density, *Aerosol Sci. Technol*. 36:227–238.

Morawska, L., Bofinger, N. D., Kocis, L., and Nwankwoala, A. (1998). Submicrometer and Supermicrometer Particles form Diesel Vehicle Emissions, *Env. Sci. Tech.* 32:2033–2042.

Park, K., Cao, F., Kittelson, D., and McMurry, P. (2003). Relationship Between Particle Mass and Mobility for Diesel Exhaust Particles, *Env. Sci. Tech.* 37:577–583.

Pierson, W. R., Gertler, A. W., and Bradow, R. L. (1990). Comparison of the SCAQS Tunnel Study with Other On-road Data, *J. Air Waste Manag. Assoc.* 40:1495–1504.

PMTACS. (2000). Available at http://www.asrc.cestm.albany.edu/pmtacsny/

Pope, C. A., Burnett, R. T., Thun, M. J., Calle, E. E., Krewski, D., Ito, K., and Thurston, G. D. (2002). Lung Cancer, Cardiopulmonary Mortality, and Long-term Exposure to Fine Particulate Air Pollution, *J. Am. Med. Assoc.* 287:1132–1141.

Prucz, J. C., Clark, N. N., Gautam, M., and Lyons, D. W. (2001). Exhaust Emissions from Engines of the Detroit Diesel Corporation in Transit Buses: A Decade of Trends, *Env. Sci. Tech.* 35:1755–1764.

Rogge, W. F., Hildermann, L. M., Mazurek, M. A., Cass, G. R., and Simoneit, B. R. (1993). Sources of Fine Organic Aerosol. 2. Noncatalyst and Catalyst-equipped Automobiles and Heavy-duty Diesel Trucks. 27:636–651.

Sakurai, H., Tobias, H. J., Park, K., Zarling, D., Docherty, K. S., Kittelson, D., McMurry, P., and Ziemann, P. J. (2003). On-Line Measurements of Diesel Nanoparticle Composition and Volatility, *Atmos. Env.* 37:1199–1210.

Sawyer, R. F., Harley, R. A., Cadle, S. H., Norbeck, J. M., Slott, R., and Bravo, H. A. (2000). Mobile Sources Critical Review: 1998 NARSTO Assessment, *Atmos. Env.* 34:2161–2181.

Schauer, J. J., Kleeman, M. J., Cass, G. R., and Simoneit, B. R. (1999). Measurement of Emissions from Air Pollution Sources. 2. C1 through c30 Organic COmpounds from Medium Duty Diesel Trucks, *Environ. Sci. Technol.* 33:1578–1587.

Shorter, J. H., Herndon, S. C., Zahniser, M. S., Nelson, D. D., Jayne, J. J., and Kolb, C. E. (2001). Characterization of heavy-duty vehicle exhaust in dense urban environments. *10th International Symposium "Transport and Air Pollution,"* September 17–19, Boulder, CO, pp. 33–40.

Stedman, D. H., Bishop, G. A., and Aldrete, P. (1997). On-road CO, HC, and Opacity Measurements. *7th CRC On-Road Vehicle Emissions Workshop*, April 9–11, San Diego, CA.

Tobias, H. J., Beving, D. E., Ziemann, P. J., Sakurai, H., Zuk, M., McMurry, P., Zarling, D., Waytulonis, R., and Kittleson, D. B. (2001). Chemical Analysis of Diesel Engine Nanoparticles Using a Nano-DMA/Thermal Desorption Particle Beam Mass Spectrometer, *Env. Sci. Tech.* 35:2233–2243.

Tobias, H. J., Kooiman, P. M., Docherty, K. S., and Ziemann, P. J. (2000). Real-Time Chemical Analysis of Organic Compounds Using a Thermal Desorption Particle Beam Mass Spectrometer, *Aerosol Sci. Tech.* 33:170–190.

Yanowitz, J., Graboski, M. S., Ryan L. B. A., Alleman, T. L., and McCormick, R. L. M. (1999). Chassis Dynamometer Study of Emissions from 21 In-Use Heavy-Duty Diesel Vehicles, *Env. Sci. and Tech.* 33:209–215.

Yanowitz, J., McCormick, R. L., and Graboski, M. S. (2000). In-Use Emissions from Heavy-Duty Diesel Vehicles, *Env. Sci. Tech.* 34:729–740.

Zahniser, M. S., Nelson, D. D., McManus, J. B., and Kebabian, P. L. (1995). Measurement of Trace Gas Fluxes Using Tunable Diode Laser Spectroscopy, *Phil. Trans. R. Soc. Lond. A* 351:371–382.

Zhang, X., Smith, K. A., Worsnop, D. R., Jiménez, J., Jayne, J. T., and Kolb, C. E. (2002). A Numerical Characterization of Particle Beam Collimation by an Aerodynamic Lens-Nozzle System. Part 1, An Individual Lens or Nozzle, *Aerosol Sci. Tech.* 36:617–631.